

## Steel-sandwich elements in bridge applications

PETER NILSSON

Department of Civil and Environmental Engineering

*Division of Structural Engineering*

*Steel and Timber Structures*

CHALMERS UNIVERSITY OF TECHNOLOGY

Göteborg, Sweden 2015

Report 2015:11



REPORT 2015:11

# Steel-sandwich elements in bridge applications

PETER NILSSON

Department of Civil and Environmental Engineering  
*Division of Structural Engineering*  
*Steel and Timber Structures*  
CHALMERS UNIVERSITY OF TECHNOLOGY  
Göteborg, Sweden 2015

Steel-sandwich elements in bridge applications

PETER NILSSON

© PETER NILSSON 2015

Report 2015:11  
ISSN 1652-9162

Department of Civil and Environmental Engineering  
*Division of Structural Engineering*  
*Steel and Timber Structures*  
Chalmers University of Technology  
SE-412 96 Göteborg  
Sweden  
Telephone: + 46 (0)31-772 1000

Cover:  
Cross section of a corrugated core steel sandwich element

Chalmers reproservice  
Göteborg, Sweden 2015

PETER NILSSON

Department of Civil and Environmental Engineering

*Division of Structural Engineering*

*Steel and Timber Structures*

Chalmers University of Technology

## ABSTRACT

Sandwich structures have been used in different applications for 100 years, since World War One. Steel sandwich elements have been proposed to be produced using an adhesive connection or discrete point spot welding. Recent increased use of and confidence in laser welding methods enables a continuous connection between the core and the face plate of a steel sandwich element. This yields a connection, and furthermore a plate element, with high strength and toughness.

The high stiffness to weight ratio and the decreased level of orthotropy in comparison to conventional stiffened steel plates, is very attractive for bridge applications. Furthermore, they have a high capacity with respect to global buckling. These properties makes sandwich plate element applicable to different bridge types, as a slab in an open cross section for short and medium span bridges or in closed box section for the stiffening girder of a cable supported bridge.

This report review's the state of art regarding steel sandwich elements in bridge applications, with a focus on the corrugated core geometrical configuration. The aim of this report is to identify the gaps of knowledge regarding corrugated core steel sandwich elements for bridge applications.

Key words: steel bridges, bridge decks, orthotropic plates, sandwich plates

## Steel-sandwich elements in bridge applications

PETER NILSSON

Institutionen för bygg- och miljöteknik

Avdelningen för Konstruktionsteknik

Stål- och träbyggnad

Chalmers tekniska högskola

### SAMMANFATTNING

Sandwichstrukturer har tillämpats för olika ändamål i 100 år, sedan första världskriget. Det har framkommit förslag att använda stålsandwichelement, sammanfogade med en elastomerkärna eller punktsvetsning. Med ökad användning av- och ökat förtroende för lasersvetsning möjliggörs tillverkning av ett sandwichelement helt i stål med en kontinuerlig fog mellan kärnan och ytplåtarna. Detta ger en svets, och vidare ett plattelement, med stor bärförmåga och robusthet.

Den höga kvoten mellan styvhet och massa och den minskade nivån av ortotropi vid jämförelse med konventionella avstyvade stålplattor, gör sandwichplattorna väldigt attraktiva för broapplikationer. Vidare har dom även en hög kapacitet med avseende på global instabilitet. Dessa egenskaper gör stålsandwichelementen tillämpbara för olika typer av broar, så som brodäck i ett öppet tvärsnitt för korta och medellånga spännvidder eller slutna lådtvärsnitt för broar med stora spännvidder.

Denna rapport sammanfattar tidigare forskning och tillämpning av stålsandwichelement för broapplikationer. Ett speciellt focus är riktat till de sandwichplattor med en korrugerad profil i kärnan. Målet med denna rapport är att identifiera de kunskapsluckor som finns gällande tillämpning av stålsandwichelement i broar.

Nyckelord: stålbroar, brodäck, ortotropa plattor, sandwichplattor

# Contents

ABSTRACT	I
SAMMANFATTNING	II
CONTENTS	III
PREFACE	V
1 INTRODUCTION	1
1.1 Background	1
1.2 Conventional orthotropic deck	2
1.3 Sandwich plates	3
2 PRODUCTION	5
2.1 Element production	5
2.1.1 Gas Metal Arc Welding	5
2.1.2 Laser welding	6
2.1.3 Hybrid laser-arc welding	6
2.1.4 Comparison of welding methods	8
2.2 Element to element joints	9
2.2.1 Geometry	10
2.2.2 Design	11
2.2.3 Manufacturing	12
3 STRUCTURAL PERFORMANCE	14
3.1 Core configurations	14
3.2 Bending behavior	15
3.2.1 Orthotropic sandwich plate theory	15
3.2.2 Core geometries	15
3.3 Mechanisms of enhancement	19
3.3.1 Stiffness to weight ratio	19
3.3.2 Level of orthotropy	20
3.3.3 Shear lag effect	21
3.3.4 Other aspects	21
3.4 Stability	22
3.4.1 Web-core sandwich plate	22
3.4.2 Truss-core sandwich beam	24
3.5 Strength	25
3.6 Dynamic response	26
3.7 Patch loading	26
3.8 Optimization	26
3.9 Design	27

4	FATIGUE PERFORMANCE	28
4.1	Laser-welded joints	28
4.2	Hybrid laser-arc welded joints	34
5	APPLICATIONS	37
5.1	Bridge slab in open cross section	37
5.1.1	General	37
5.1.2	Case study	37
5.2	Box girder cross section	40
	REFERENCES	42

## **Preface**

This is a pre-study for a research initiative from the research group of steel and timber structures at Chalmers University of Technology. It concerns steel sandwich elements and their application in bridges and it is intended to review the state of art. It was performed during September to December of 2014. Statens Vegvesen was the initiator and founder of this project. The study was performed in collaboration with WSP. The author would like to thank the following persons for their contribution to this work.

Mohammad Hoseini, Statens Vegvesen

Mathias Eidem, Statens Vegvesesn

Roland Olsson, WSP

Tore Roppen, Kleven verft AS

Sören Ehlers, Hamburg University of Technology

Peter Nilsson

Göteborg, 2015-09-09



# 1 Introduction

## 1.1 Background

In 2013 the world produced over 1.6 billion tons of crude steel [1]. The need to produce innovative light-weight structures that utilize the material efficiently is of great interest with regards to our CO<sub>2</sub> foot-print, in multiple aspects. Annual usage of crude steel in the world is shown in Figure 1.

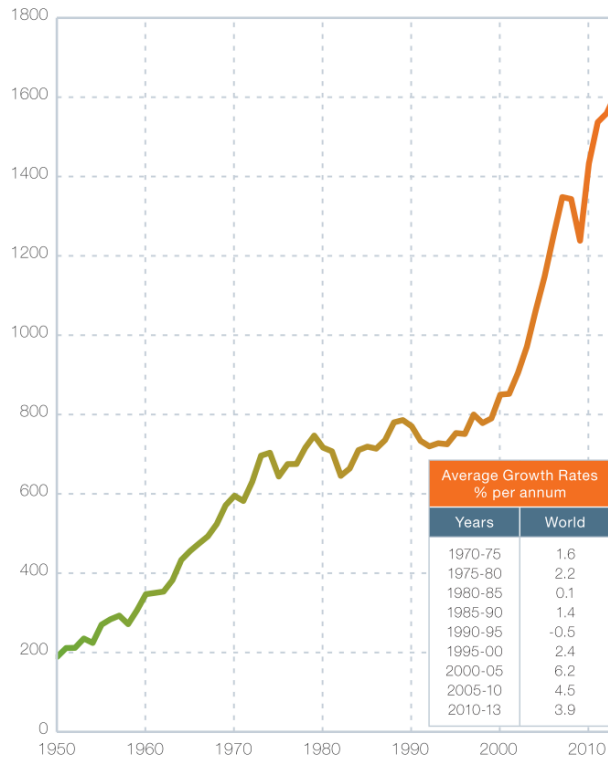


Figure 1 Annual consumption of steel in the world [1].

Bright and Smith stated that since the 1970's the design of orthotropic steel-decks has remained principally unchanged [2]. The conventional orthotropic steel-deck that is used in bridge applications generally consists of a top steel plate and longitudinal closed or open stiffeners (see e.g. Wolchuck [3]). Bright and Smith also state that this type of bridge decks has suffered from extensive fatigue damage due to their complex details and sensitivity to local loading [2]. The highly orthotropic behavior increases the stress levels in these regions. With future increase in traffic loads this issue will be more critical. A promising concept as a substitute for the conventional orthotropic plate is the all steel-sandwich element (aSSE). This is a light-weight high-performing orthotropic plate element. It consists of a top and a bottom plane steel plate, separated by a low-density core element. Steel sandwich elements can be potentially used in several bridge related applications, some of which are:

- As orthotropic steel deck in all-steel bridges with open cross section,
- Assembling sandwich elements to form a box-girder for long span bridges,

- Re-decking of degraded concrete decks in existing composite (steel-concrete) bridges, carrying loads without longitudinal composite action.

These three possible bridge applications are shown in Figure 2.



Figure 2:     *left:*             *steel sandwich deck in all-steel girder bridge [5]*  
                   *middle:*            *box girder cross section [6]*  
                   *right:*             *re-decking of bridge [4]*

Even though the concept of steel sandwich plates was considered already back in the 1950s, the production of such elements became feasible only recently through new and improved welding technologies. These production methods also start to reach the point to give economically sustainable solutions.

Introducing modern welding techniques not only allowed new structural configurations that are high-performing with a long estimated life, but also increased the level of automatization in production. In times of rapid salary-increases, (see e.g Kenno Tech [7]) this increases the competitive possibilities for local production in high-salary regions.

There exist different proposals for the use of sandwich elements in bridge applications. For example, the product with two face steel sheets and an elastomer core, shown and evaluated in SANDCORE [8]. This report mainly refers to the aSSE, as it is robust, stated by SANDCORE [8], and has the advantage of utilizing only steel as a structural material, which has well defined commonly known mechanical properties.

## 1.2 Conventional orthotropic deck

The conventional orthotropic steel deck consists of a plane top steel plate, stiffened by longitudinal open or closed stiffeners. Closed trapezoidal stiffeners are used to increase the local torsional stiffness of the plate, stated e.g. by Wolchuck [3]. The main purpose of this secondary load-carrying element is to transfer the locally applied vertical forces to the transverse beams and from there to the main longitudinal girders. Conventional orthotropic bridge decks have a very high degree of orthotropy due to the large ratio of longitudinal to transversal bending stiffness. Kolstein states that they are often used where a low structural weight is the driving force in the design [9], such as movable bridges and long-span cable-supported bridges.

The longitudinal stiffeners in orthotropic decks are continuous elements passing through cut-outs made in the transverse girders. The stiffeners can either be welded all-round or the orthogonal element can have a cutout under the lower horizontal part of the stiffener, as in Figure 3 that displays the cross section of a conventional stiffened plate.



Figure 3. Cross section of conventional orthotropic steel deck [5].

Fatigue damage is a common problem in orthotropic bridge decks. They can occur in various details, such as the welded detail between the stiffener and the deck plate (see e.g. Bright and Smith [2]) and the welded connection between stiffeners and transversal beams. In the former case, the cracks can arise either in the deck plate or the stiffeners web. Wolchuk showed that fatigue cracks can also occur in the deck to cross-girder joint [10]. These fatigue cracks arise due to the complexity of the detail and are amplified by the high level of orthotropy in the structure.

Kolstein made an extensive review of the research made in the field of orthotropic plates. Among other recommendations, Kolstein suggested geometrical demands for the welded connection between the deck plate and the web of the stiffener, to avoid a lowered fatigue strength [9]. Figure 4 shows possible crack positions in stiffener to deck plate joint.

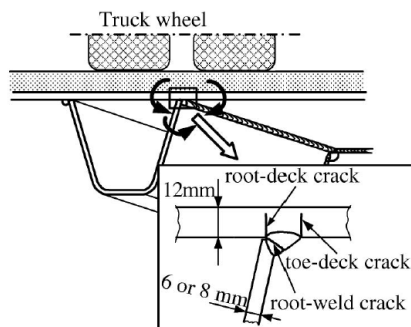


Figure 4. Fatigue cracks in orthotropic deck [11].

Beneus and Koc stated that the main research proposals for enhancing the fatigue strength of this element was to increase plate thicknesses [5].

### 1.3 Sandwich plates

A sandwich element is a plate structure defined by stiff surface plates separated by a light-weight core. The basic idea is that the surfaces plates carry loads in bending action while the core carry load in shear action.

The “sandwich effect” is explained as an increase in bending stiffness when separating the face sheets by a low density core and simultaneously minimizing the weight increase (see e.g. SANDCORE [8] or Säynäjäkangas and Taulavuori [12]). This effect is illustrated in Figure 5. It can be seen in Figure 5 that separating the face-plates by a

distance equal to the thickness of the face plates will increase the flexural stiffness with a factor of 7.

	Solid Material	Core Thickness $T$	Core Thickness $3T$
Stiffness	1.0	7.0	37.0
Flexural Strength	1.0	3.5	9.2
Weight	1.0	1.03	1.06

Figure 5. Illustration of the “sandwich effect” [8].

The first proposals regarding the steel-sandwich element (SSE) dates back to the 1950’s, (see e.g. Kujala and Klanac [13]) and was at that time meant for aerospace applications. Bright and Smith [2], and Hoffart and Hansen [14] told that the proposed innovative concepts were though not possible to produce with a continuous joint between the core and the face plates using conventional welding available at that time. Figure 6 shows some different geometries for aSSE’s.

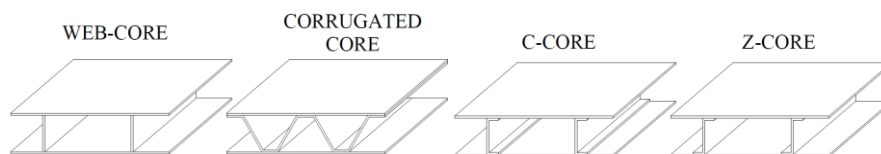


Figure 6. Various configurations of steel sandwich elements [15].

Production methods available today, such as laser welding, enables the production of the geometric configuration of a SSE, stated by e.g. Bright and Smith [2]. Alwan and Järve declare that the use of SSE’s started to increase about 20 years ago [16]. Development of the structural element is at present driven mainly in the marine sector. Material savings up to 50% are presented by many authors when comparing SSE’s to conventional solutions, see e.g. Bright and Smith [2], Beneus and Koc [5], Kujala and Klanac [13], Roland and Reinert [17] and Kujala et. al. [18].

A SSE that has shown potential according to Beneus and Koc [5], Alwan and Järve [16], and Biagi and Bart-Smith [19] is the configuration with a corrugated core. Caccese and Yorulmaz declare that this is not only by stiffness-to-weight ratio, but also with regards to production ability [20]. The corrugated core sandwich cross sectional configuration is shown in Figure 7.

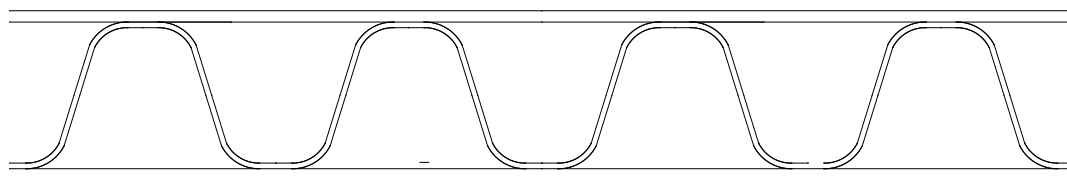


Figure 7. Corrugated core steel sandwich cross sectional configuration.

## 2 Production

This section regards the production of SSE's. Element production is regarding welding methods used to assemble steel plates into a sandwich plate and the element to element assembly is regarding the methods of joining elements to each other.

### 2.1 Element production

The limiting factor for SSE's has historically been the production process. It demands single-sided welding. The weld type needed to assemble an SSE is called a through thickness stake weld, see Figure 8.

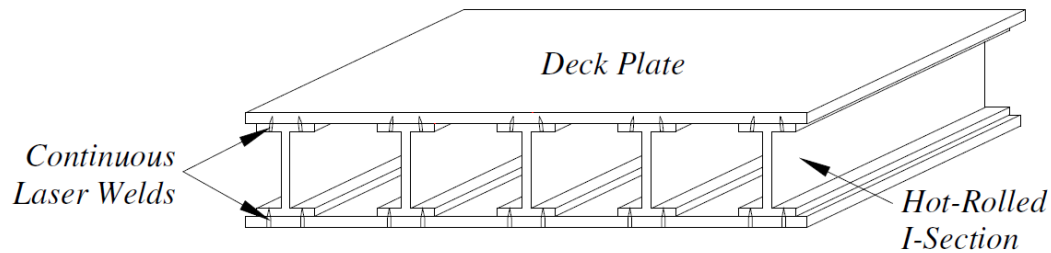
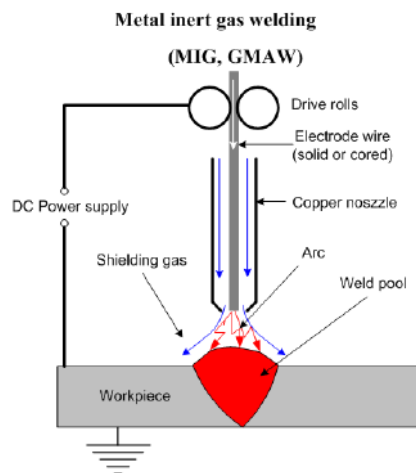


Figure 8. Through thickness laser stake weld in sandwich with rolled I-section core [2].

For infrastructure applications, such as bridges, penetration of relatively thick plates needs to be considered. Therefore, SSE's place high demands on the production, such as using modern welding techniques, performed in a modern steel-shop.

#### 2.1.1 Gas Metal Arc Welding

The Gas Metal Arc Welding (GMAW) technique is mentioned here due to its coupling to hybrid welding methods. It is based on continuous deposition of molten electrode material on to the base material creating a weld pool (see e.g. Baker [21]). Figure 9 shows a schematic sketch of the principle of GMAW.



[www.substech.com](http://www.substech.com)

Figure 9. Gas Metal Arc Welding [22].

Key advantages of GMAW are that it is an affordable production method, without any slag removal and with a high weld quality. The disadvantage is that it yields a wide weld when deep penetrations are needed. The energy density of the electric arc is not high enough to perform a trough thickness stake weld by GMAW alone. This production method can be either semi- or fully automatic. Semi-automatic production methods are often used when assembling an orthotropic bridge deck. The manual part of this method may introduce local irregularities in the weld, leading to a risk of initiating a fatigue crack.

### **2.1.2 Laser welding**

Laser welding (LW) is a possible production method available today, when considering assembly of SSE's. Other methods are under development, e.g. cathode-focused tungsten inert gas welding, but currently they are not available for production, for the regarded purpose.

Denney reported that laser beam welding was developed in the 1960's, and has been used in fabrication from the 1990's [23]. The process of LW is highly industrialized and automatized, see e.g. Jefferey et. al. [24]. In the report SANDWICH it was stated that this is a rapid production process and it decreases production time with 30% for the case of fabrication of marine vessels [25]. Panels are assembled and welded by robots, then transported to a new site for element-to-element assembly. Lankalaoalli presented a model for estimation of the penetration depth [26]. The penetration depth of a laser welded connection is dependent on the propagation speed of the welding process shown e.g. by Lankalaoalli [26]. As the energy density of the LW is high and the weld speed is high, the heat affected zone (HAZ) becomes small. This has been stated by many authors, see e.g. Bright and Smith [2]. This yields low residual stresses, low distortions, and small initial deformation, all of which enhances the buckling and fatigue strength of the welded elements.

No filler material is required for LW (see e.g. Miller [27]).

### **2.1.3 Hybrid laser-arc welding**

The combined process of LW and GMAW is called hybrid laser-arc welding (HLAW). Hoffart and Hansen declared that the two technologies are combined to utilize their unique strong features [14]. Together they create a robust connection with a long service life. The laser component of the hybrid performs the large penetration depth with a small HAZ and the arc welding component improves impurities, joint-root openings and increases the control factor, see Hoffart and Hansen [14] and Defalco [28]. The principle of this welding technique is displayed schematically in Figure 10.

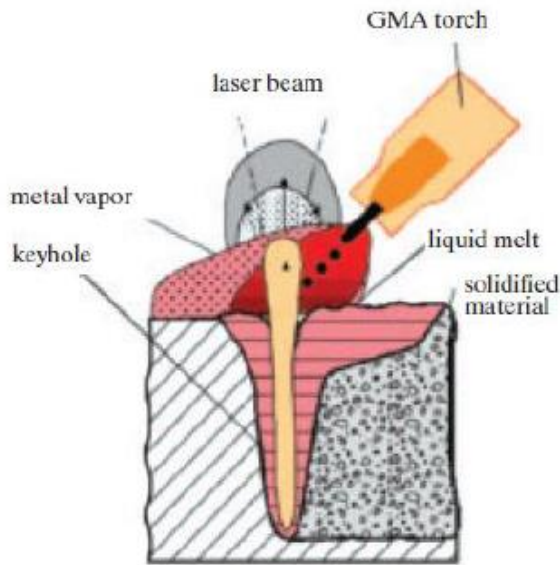


Figure 10. Principle of HLAW [28].

Hoffart and Hansen stated that based on test results, these welds perform as well as, or better than conventional welds, in all aspects [14].

An investigation of the current commercial use of HLAW was conducted by Beneus and Koc. It was stated that by early 2014 approximately 100 HLAW units are in use worldwide. 40 of them are installed in Germany and no units in Sweden. The modest use of HLAW was stated to be due to high initial costs, that for the laser unit was about 500' SEK per kW of laser power [5].

The relation between laser power, penetration depth and weld speed is displayed in Figure 11. It can be seen that a high laser power and low welding speed increase the penetration depth.

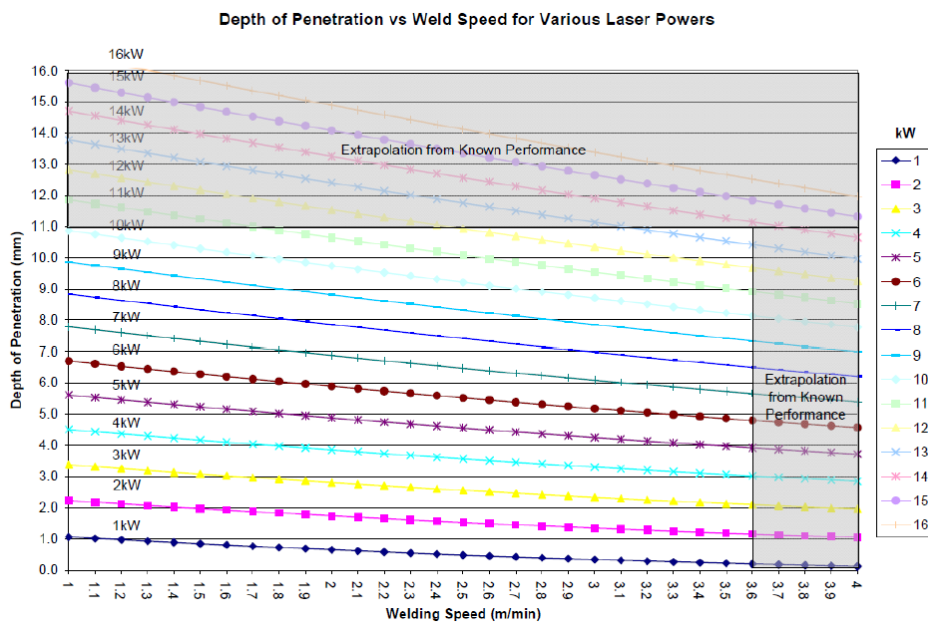


Figure 11. Relation between laser power, penetration depth, and weld speed for HLAW [29].

### 2.1.3.1 Residual stress

Residual stresses induced by an uneven distribution of temperature related contractions during solidification of the weldment is an important factor for stability and fatigue.

Wenzel et. al. tested butt-welds using HLAW for thick plates of 40 mm. It was shown that tensile residual stresses were decreased in comparison to conventional methods and that this had a positive effect on the fatigue strength [30].

Abbot et al. state that the residual stress level in joined plates generally is lower when using HLAW compared to conventional welding techniques [31].

### 2.1.4 Comparison of welding methods

Jefferey et. al. stated that apart from high welding speed and reduced residual stresses, LW also gains from ease of process automation, high productivity, increased process reliability and low distortion in comparison to conventional welding [24].

HLAW is up to 10 times faster than conventional welding, declared e.g. by Hoffart and Hansen [14], and Caccese and Yorulmaz [20].

LW and HLAW are compared to conventional welding by Alwan and Järve [16]. Figure 12 displays the differences in terms of welding speed, possible plate penetration depth (thickness), maximum weld gap and distortions. Figure 13 visualizes the general weld profile of the three discussed weld types.

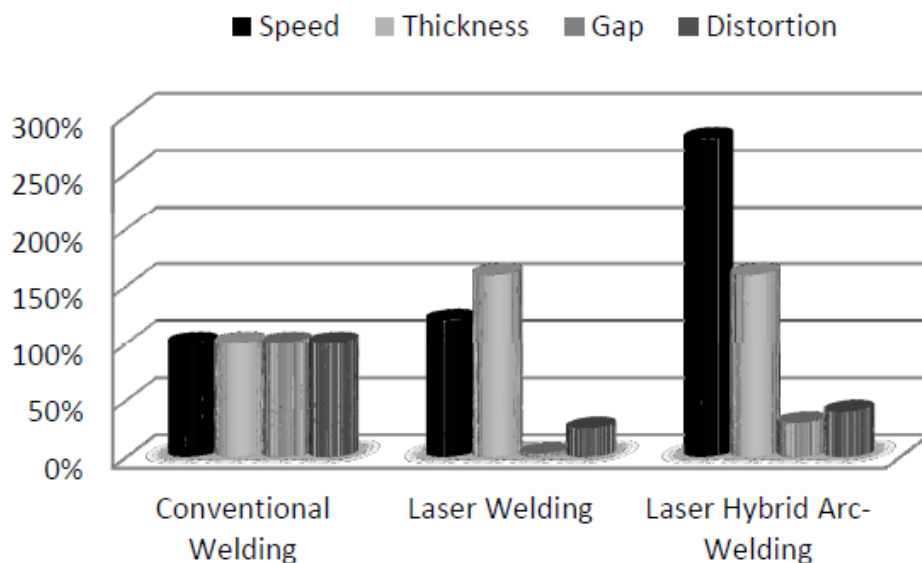


Figure 12. Comparison of welding techniques [16].

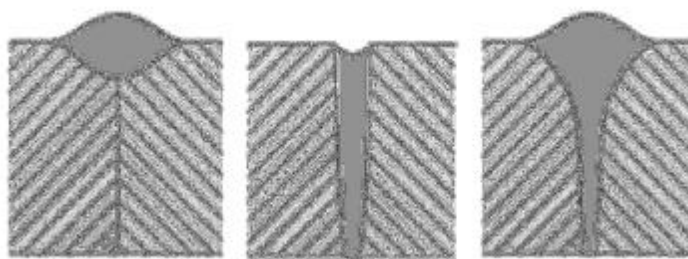


Figure 13. General geometrics of welds, GMAW (left), LW (middle) and HLAW (right) [16].

Wetzel et al. [999] compared three methods for performing a butt-weld in 40mm plates: (a) two-sided submerged arc weld of 5 –7 passes per side; (b) single-sided hybrid weld in the root, filled with 2 –3 passes of submerged arc weld per side; and (c) double-sided hybrid-weld in the root, filled with 2 –3 passes of submerged arc weld per side. This study showed an economical gain of 20% for the combined submerged arc hybrid laser welding processes over the submerged arc method solely [30].

Furthermore Wetzel et al. compared the penetration depth and input energy of GMAW, LW and HLAW. In Figure 14 it can be seen that LW gives a larger penetration depth than GMAW with the same power input. It can also be seen that HLAW increases the penetration depth further, to the cost of higher power input [30].

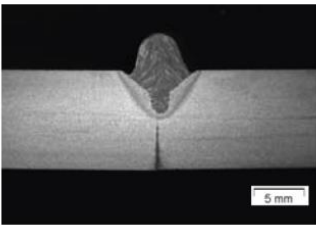
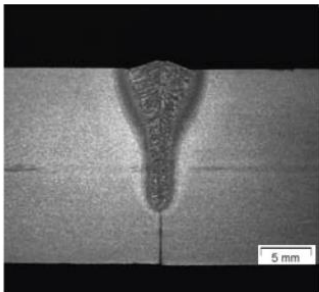
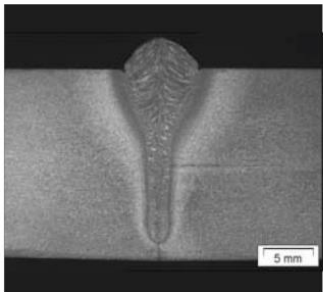
Arc, stand-alone	Laser, stand-alone	Hybrid
		
Arc power 11.28 kW	Laser power 12 kW	Arc power 11.28 kW Laser power 12 kW
Penetration depth 4.4 mm	Penetration depth 13.97 mm	Penetration depth 19.48 mm

Figure 14. Penetration depth and energy input [30].

## 2.2 Element to element joints

There are two different types of joints to consider regarding joining of two SSE's:

- Parallel to the direction of the corrugation
- Perpendicular to the direction of the corrugation

In this section, *all knowledge is from the ship building industry.*

SANDCORE reviewed best practice of sandwich structures in marine applications, it was stated that the following joining techniques can be adopted for all-metal or metal-hybrid sandwich elements [8]:

- Welded joints
- Mechanically fastened joints
- Adhesively bonded joints
- Combined joints

It was also declared by SANDCORE that welded connections are most commonly used [8].

## 2.2.1 Geometry

It was stated in SANDCORE that due to the relatively thin face sheets (typically 2-4 mm in web-core sandwich plates for marine applications [32]), a joining element is normally used [8]. Furthermore it was concluded that welded connections between the plate element and joining element are the most common [8]. In Figure 15 a typical joint, perpendicular to the direction of the corrugation, of an aSSE for marine purpose is shown.

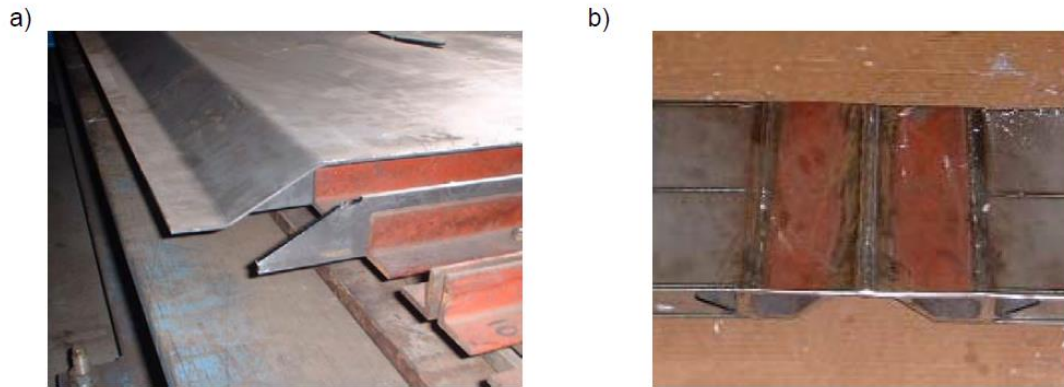


Figure 15. Joint in production (left) and joint in panel (right) [8].

A set of considered sandwich joints for ship utilization purpose is shown in Figure 16 with red marks for stress-intensive points.

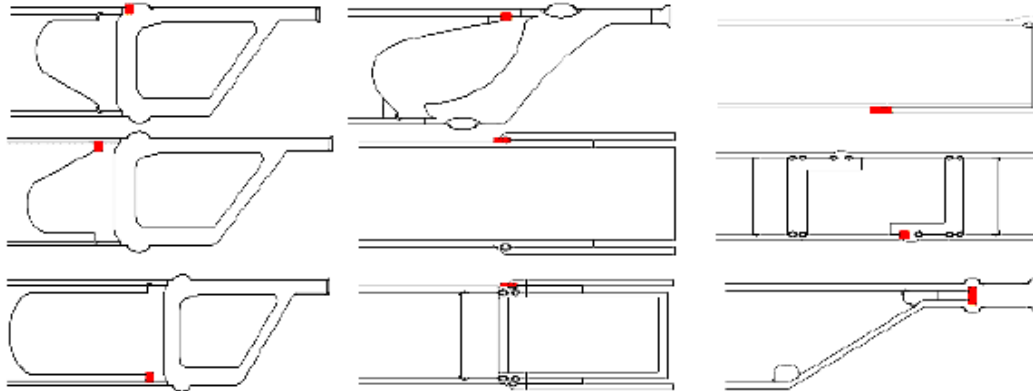


Figure 16. Sandwich joints and red-marked stress intensive locations [8].

Karol [xx] searched for an optimum joint geometry for a longitudinal panel-to-panel joint in his work. The focus of the comparative research was to minimize geometrical stress concentrations. Considered joint and proposed connection solutions are shown in Figure 17. The optimal solution was shown to be the rectangular profile of Figure 7, type b), in terms of stress levels. It was though not the lightest solution [33].

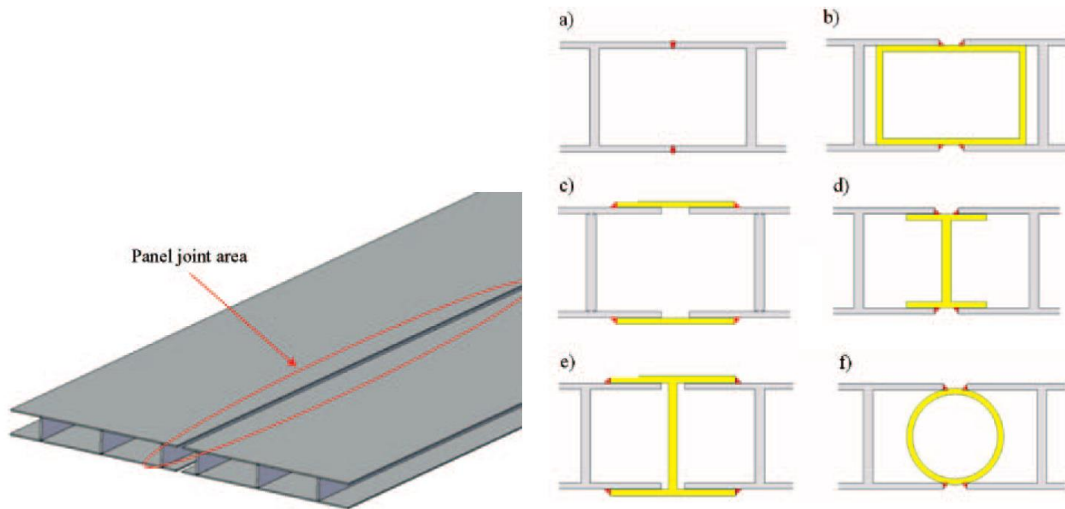


Figure 17. Longitudinal element to element joint (left) and proposed solutions (right) investigated by Karol [33].

Kozak [xx] briefly discussed the case of angularly joined sandwich elements. Two types of connections were proposed and they are shown in Figure 18 [34].

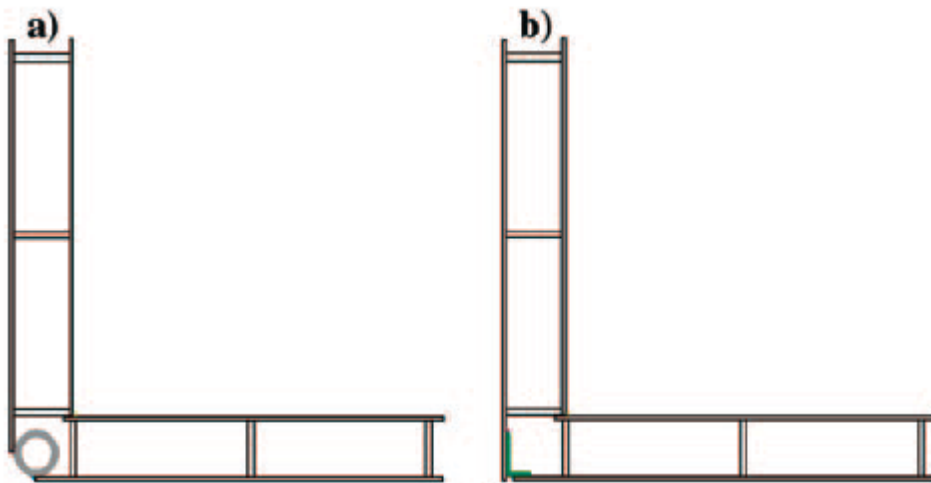


Figure 18. Proposals for angular panel to panel joints [34].

### 2.2.2 Design

SANDCORE presented an outline for proper designing of a sandwich element joints is shown in Figure 19.

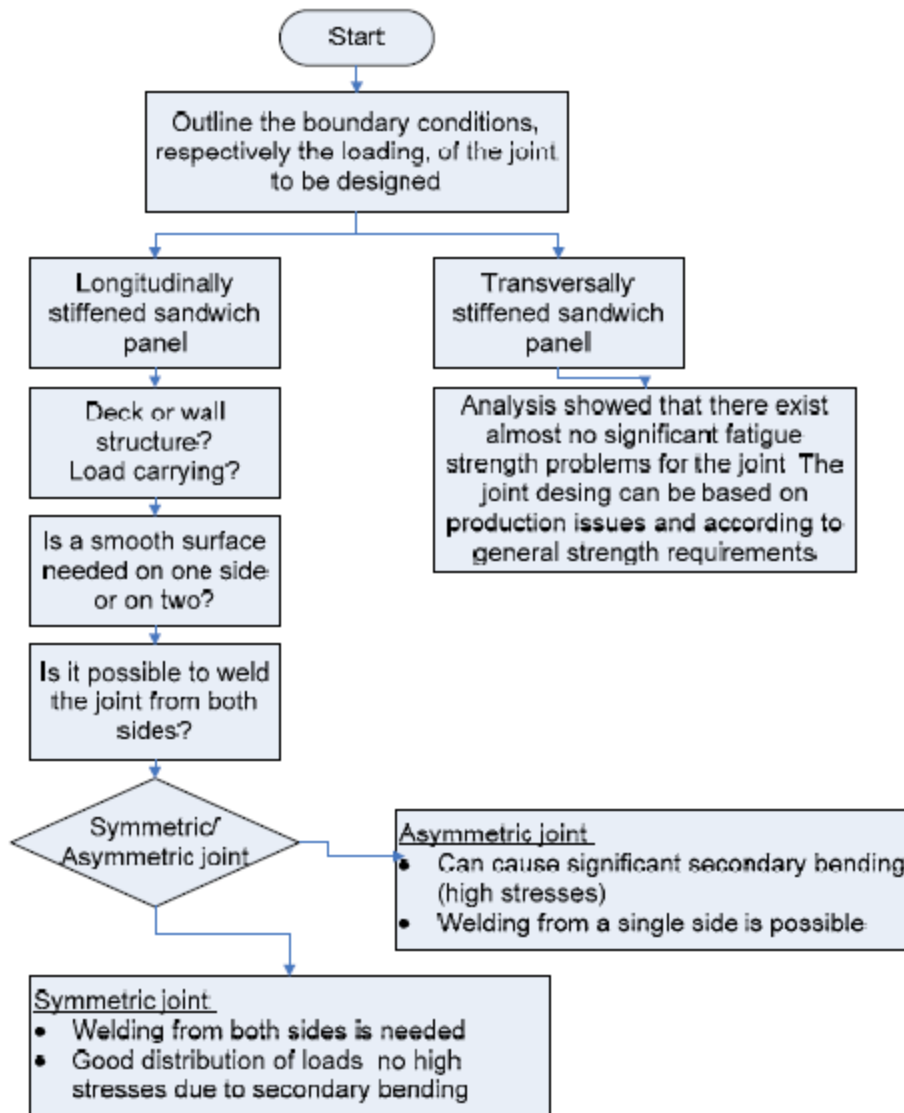


Figure 19. Flow chart for proper design of sandwich joint [8].

It was stated by Kujala and Klanac [xx] that the main design topic regarding sandwich joints is fatigue. Furthermore they declared that there are no fatigue design-catalogues available for steel sandwich element joints at the present [13].

### 2.2.3 Manufacturing

A joint shall be designed to fulfill the requirements for its life-time performance. However, the production process needs to be considered. Recommendations regarding the production process were given by SANDCORE and are quoted below [8].

- Although the pre-manufacturing accuracy of all-metal sandwich panels is usually high, there may be some global distortions in the case of large panels (local distortions rarely appear before assembly). Such distortions can complicate the joining of panels. In order to assist the easy fitting of adjacent panel edges, it is

recommended, where possible, to place panel joints on supporting longitudinal girders or transverse beams. Common mechanical devices can then be used to press the panels down to the girders and fit them.

- A general design principle is to try to prevent the transfer of global loads to sandwich structures. This can be easily achieved for applications such as sun decks or moveable ramps, and makes the sandwich joints more straightforward and less costly to assemble.
- Tolerance-friendly joints (e.g. tongue and groove) help to accommodate the dimensional tolerances of sandwich panels and, more importantly, the surrounding ship structure, thereby minimising costly fitting work.
- In order to avoid global distortions due to welding during panel fabrication and assembly, a minimum moment of inertia is recommended for sandwich panels. This is most readily achieved by ensuring that the overall thickness of a sandwich panel is sufficiently high. For example, based on the experience of using I-Core sandwich panels in the decks of inland waterway cruise ships, Meyer Werft recommends a minimum stiffener height of 40 mm.

### 3 Structural performance

#### 3.1 Core configurations

The structural behavior of steel sandwich element is similar to that of an I-girder. Bending stiffness is achieved by the distanced outer flanges and the core limit the shear strains. A relevant property, in terms of load distribution and over-all bending stiffness, is the level of orthotropy. This is determined by the core configuration.

Figure 20 and Figure 21 show a range of alternatives regarding core geometries.

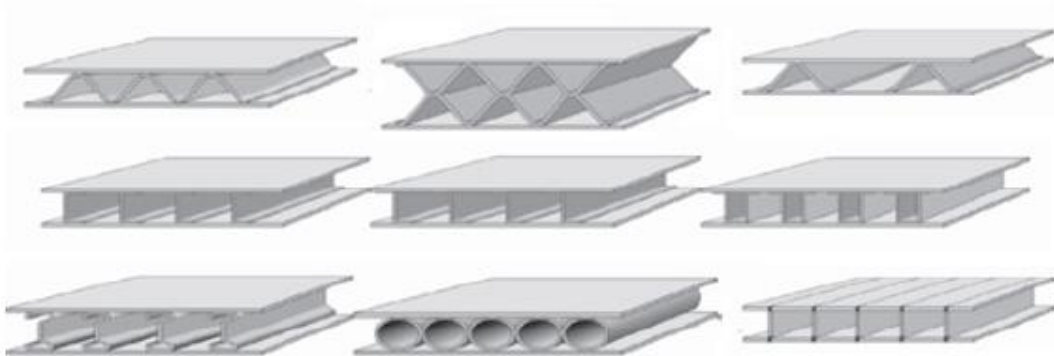


Figure 20. Various core configurations [35].

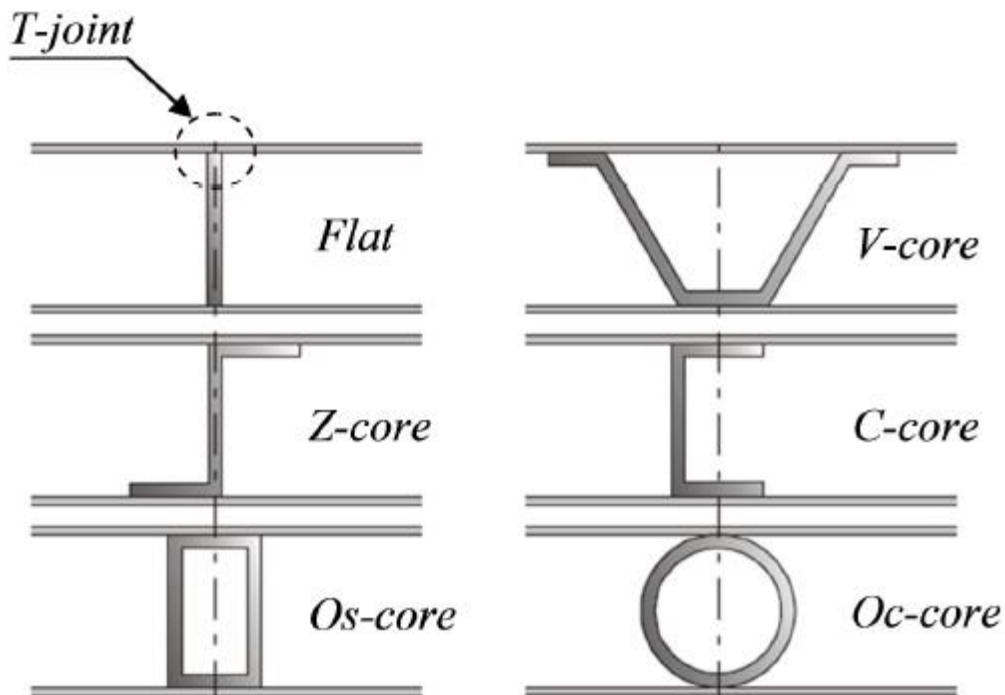


Figure 21. Name of core types [16].

## 3.2 Bending behavior

### 3.2.1 Orthotropic sandwich plate theory

All types of aSSE's have a core which is connected to the face plates in discrete positions, lines in the longitudinal direction of the core. The SSE is not homogenous. To analyze the 3D SSE as a single plate structure, it needs to be homogenized, i.e. cross sectional constants for determining average response is needed. Homogenization will strongly reduce the numbers of unknowns in a plate analysis whether it is analytical or numerical. Reducing a structural problem in this manner decreases the computational time to the cost of a non-complete result.

In 1948 Libove and Batdorf presented a small deflection theory for sandwich plates based on Reissner-Mindlin kinematics where the contribution of shear deformations to the deflection was accounted for [36].

Romanoff and Varsta stated that homogenized orthotropic sandwich theories cannot fully predict a shear-induced secondary bending moment [37]. This effect induces bending stresses in the face plates in the direction perpendicular to the core under shear action. Furthermore it was declared by Romanoff that the local stresses from a directly applied load cannot be predicted [15], i.e local behavior is not approached by the sandwich theory developed by Libove and Batdorf [36].

Regarding web-core SSEs Romanoff and Varsta developed a method of analysis to predict the average bending behavior of a sandwich plate using homogenized orthotropic plate theory. In this method the shear-induced secondary bending moment contribution to the stress prediction of the face plates was considered [37]. The method uses both analytical and numerical components in its solution. Romanoff et al developed this method further to include the effect of locally applied force [38].

This type of full stress prediction theories are not available for other core configurations.

### 3.2.2 Core geometries

This sub-chapter aims at displaying the individual core-geometries structural properties. Their produce-ability is also touched upon.

#### 3.2.2.1 Web-core

Web-core sandwich elements consist of a flat web plate as a core stiffener, see figure 22. As minimal material is used for the core the stiffness-to-weight ratio is high, when stiffness is regarding bending stiffness in the longitudinal direction of the core. The shear stiffness in the transversal direction to the core is low, which yields a high level of orthotropy and a lowered over-all bending stiffness.

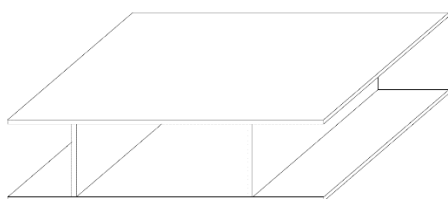


Figure 22. Web-core steel sandwich element [15].

The joint connecting the face-plates and the core in a web-core steel sandwich element is a T-joint, see Figure 23.

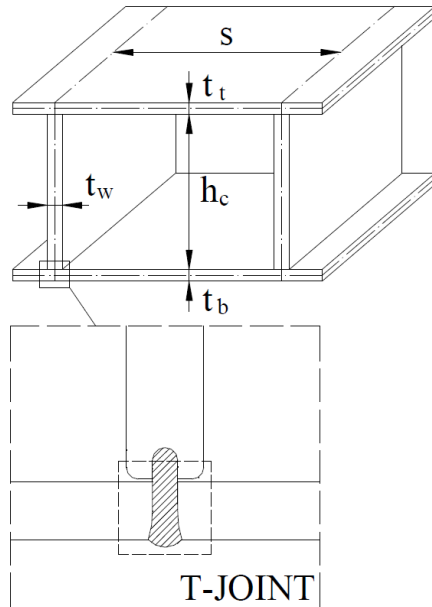


Figure 23. T-joint of a web-core steel sandwich element [15].

The width of the weld is smaller than the web-plate thickness and the laser welding induces a small gap between the welded plates. This weld rotational stiffness affects the transverse shear stiffness. An expression for transverse shear stiffness in the transversal direction including weld rotational stiffness was presented by Romanoff et.al in [39]. Furthermore the rotational stiffness of laser welded T-joints was determined statistically by experimental analysis.

### 3.2.2.2 Corrugated core

A cross section schematic of a corrugated core SSE is shown in Figure 24.

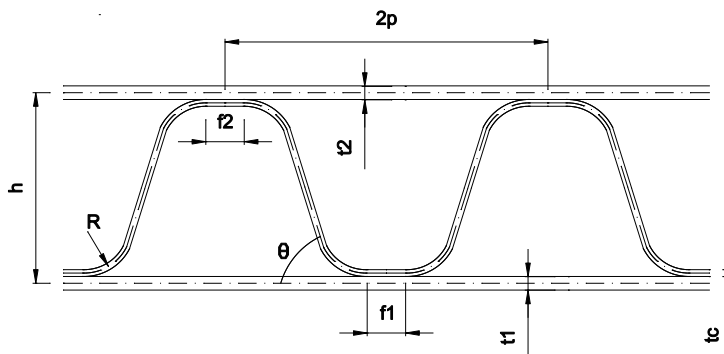


Figure 24. Corrugated core steel sandwich element cross section.

In 1951 Libov and Hubka derived elastic constants for the corrugated core sandwich element [40]. The elastic constants are shown in Appendix A for the case of symmetry around the center plane.

Chang et al. presented a closed form solution using the Mindlin – Reissner plate theory and validated by experimental analysis for different boundary conditions under uniformly distributed vertical loading [41]. This was performed for a corrugated core SSE. The model included transverse shear deformation and was based upon cross sectional constants from Libove and Hubka [40].

Also investigations by Lok and Cheng [42] and Tan et al [43] show good mean deflection estimation when using a homogenization approach.

An inclination of the core plate, as in the case of the corrugated core, yields an increase of the transversal shear stiffness in the direction perpendicular to the core, shown by many authors, e.g. Alwan and Järve [16], Lok and Cheng [44] and Chang et al [41]. Although the longitudinal bending stiffness is slightly decreased using an inclined web, this decreases the level of orthotropy and increases the over-all bending stiffness.

The transversal shear stiffness in the direction perpendicular to the core derived by Libove and Hubka assumed a single ridged link connecting the core and the face plates [40]. Analogous to the web-core steel sandwich the corrugated core has a deformable joint at the position of the assumed ridged link. Caccese and Yorulmaz investigate both the impact of the stiffness of the connecting element and the impact of multiple welds per horizontal part of the core [20]. In their full 3D numerical analyses the connection was modelled using a single standing 8-node shell element between the centerlines of the core and the face plate. This was made for a single corrugated core SSE cross section geometry and a single width and length of the plate. The cross section considered is shown in Figure 25 and the structure was in all analyses subjected to a distributed load.

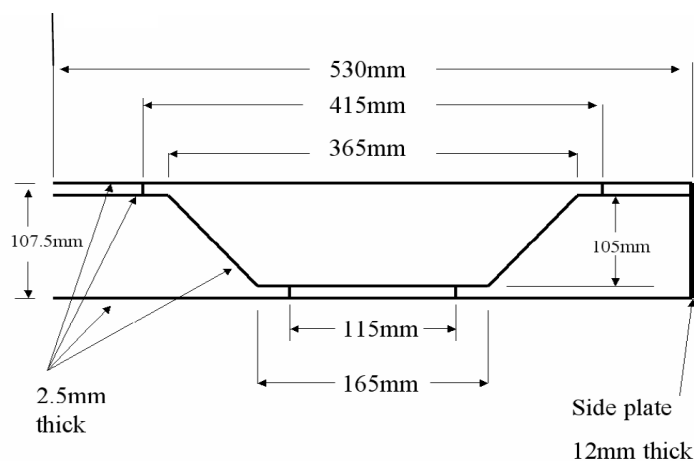


Figure 25. Considered cross section geometry of [20] for the case of two welds per horizontal part of the core.

The analysis regarding the joint link stiffness was performed using one link at the middle point of the horizontal part of the core. The result is shown in Figure 26 where it can be seen that a joint thickness between 0.5 to 50 times the plate thicknesses yields small differences in the overall deflection [20].

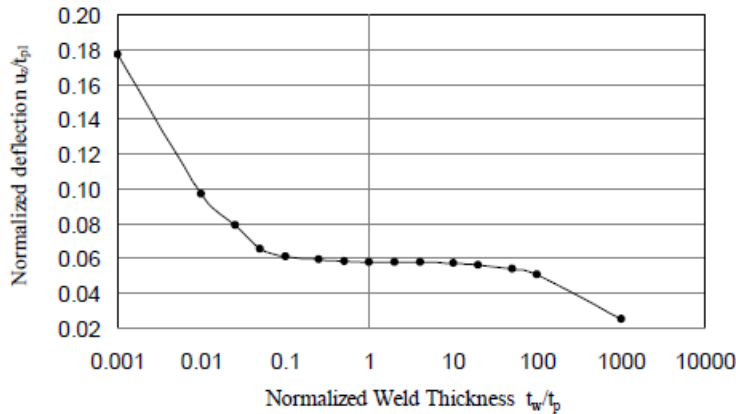


Figure 26. Impact on global deflection by increased stiffness of the weld connection [20].

Regarding the impact of the number of weld connections per horizontal part of the core a 22% difference in global deflection was shown by comparison in the bottom flange. In the top flange the difference was 66%, including the effect of local deformation. The difference was between the case of one centered connection and the case with one centered connection and one connection at each end of the horizontal part, i.e. three connections per horizontal part of the core [20]. The results of Caccese and Yorulmaz [20] shows a need for an expression of the transversal shear stiffness in the direction perpendicular to the corrugation elongation when using multiple weld beads. The impact of weld rotational stiffness when using a single weld bead is shown to be small in this single case, but further investigation is needed to exclude its impact.

No found research shows the impact of the geometric properties of a corrugated core sandwich element when subjected to bridge loading, i.e. out-of-plane bending, in-plane shear and axial compression simultaneously.

### 3.2.2.3 Other types

A triangulated core, or truss-core, has been shown to have a good over-all bending stiffness, e.g. by Alwan and Järve [16] and Cheng et. al. [45]. The triangulated core is shown in Figure 27. In similarity to the web-core sandwich element, this needs to be welded at an exact position. A position that is not visible from the position of welding. Caccese and Yorulmaz state that this geometric configuration lacks in production possibilities [20]. Alwan and Järve instead recommended a corrugated core with the horizontal part kept as short as possible, to gain maximal bending stiffness and support the production aspects simultaneously [16].

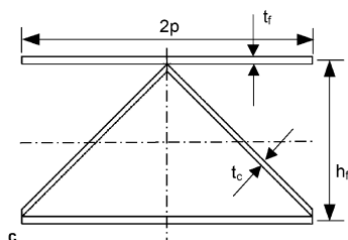


Figure 27. Triangulated core sandwich [45].

The sine-cored SSE, shown in Figure 28, was considered by Alwan and Järve and shown to have good overall bending stiffness [16]. It was not recommended due to production reasons.

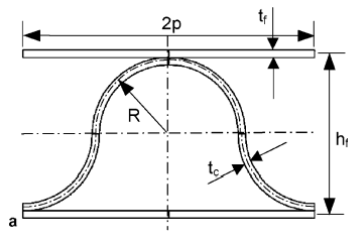


Figure 28. Sine-core sandwich [45].

Alwan and Järve stated that the X-core, see Figure 29, has a high energy absorbing capacity [16], but includes an extra folded core sheet, which affects the production cost.



Figure 29. X-core sandwich [35].

Pantsar performed a comparative study regarding core geometries, it was shown that an O-core has less initial deformations due to welding, compared to a V-core. It was also shown to have a high nominal stiffness, affecting the welding procedure. It though consumes a large core cross sectional area, reducing the stiffness to weight ratio [46].

It was also suggested by Bright and Smith that hot-rolled I-sections can be used as a core configuration, reducing production costs [2].

### 3.3 Mechanisms of enhancement

The geometry of the SSE yields enhanced structural performance to a bridge structure when the SSE is utilized as a deck. This in comparison to conventionally used plate structures. These mechanisms of enhancements is the focus of this sub-chapter.

#### 3.3.1 Stiffness to weight ratio

The SSE has a high stiffness to weight ratio in the longitudinal direction of the core, shown by many authors, e.g. Bright and Smith [2], Beneus and Koc[5] and Alwan and Järve [16]. This is achieved by keeping the center of gravity close to the center of the cross section and utilizing the face-plates efficiently with regards to bending. This is also known as the “sandwich effect”.

Thus, for many cases, when comparing a SSE to a conventional stiffened plate, the cross sectional area can be reduced while the bending stiffness is equivalent (or the other way around, equal area and increased bending stiffness). In Figure 30 the two compared cross sections are displayed.

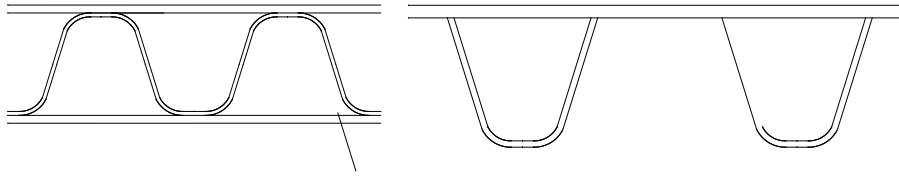


Figure 30. Cross sectional geometry of a SSE (left) and a conventional stiffened plate (right).

The high stiffness to weight ratio affects the bending capacity and the capacity in axial compression of a SSE.

### 3.3.2 Level of orthotropy

In the conventional orthotropic steel bridge deck a very high level of orthotropy is obtained. The longitudinal stiffeners carry the patch loads to its support locally. The bottom face plate of the SSE yields a structural behavior of the plate closer to that of an isotropic plate. The bending stiffness in the direction transversal to the direction of the corrugation is increased largely. Isotropic behavior is optimal with regards to bridge applications. It yields positive effects in terms of load spreading. It also induces a possibility to reduce the number of transversal supports, i.e. cross girders or diaphragms. The load distributional behavior is displayed schematically in Figure 31.

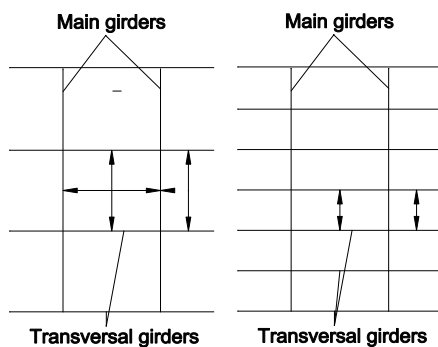
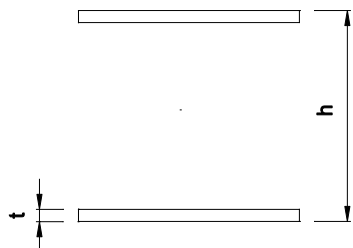


Figure 31. Load distributional behaviour of a SSE (left) and a conventional stiffened plate.

In Table 1 a calculation example comparing the bending stiffness in the transversal direction of a conventional stiffened plate and a SSE with thicknesses relevant for a bridge applications is shown.

Table 1. Transversal bending stiffness comparison of conventional stiffened plate and SSE.

	Conventional stiffened plate	SSE
		
t [mm]	16	8
h [mm]	-	140
Bending stiffness	1	~180

### 3.3.3 Shear lag effect

Shear lag effect regards the membrane stress distribution in the flange of a beam under bending action of the cross section. The distribution is dependent on the axial- and in-plane shear -stiffness of the flange plate. In-plane shear stiffness of the SSE is high which yields a high spread of normal membrane stresses in the flange, i.e. a favorable performance with regards to shear-lag effects. This gives a high global bending stiffness when the SSE is utilized as a flange plate. The effective width contributing to the bending stiffness is large. In the case study by Beneus and Koc this increased performance was shown for the case of a bridge deck, contributing to a large weight reduction [5].

Romanoff investigated different modelling techniques of a web-core SSE utilized as a flange in a beam cross section. The study showed that a different effective width was gained in the top- and bottom face sheets. It was also shown that the normal stress distribution is highly dependent on whether the core longitudinal direction coincides with the normal axis of the beam or not. The two modelling techniques tested, beam girder with sandwich slab, and shell element modelled girder with sandwich slab, showed conforming results [47].

### 3.3.4 Other aspects

There exist other aspects that enhance the structural efficiency of SSEs like residual stress level, fatigue performance or buckling strength. They are either a result of the three above mentioned aspects or not related to the cross section geometry, and are treated separately.

### 3.4 Stability

When an aSSE is utilized in a bridge application, for example as a slab in a movable bridge, or top plate in a stiffening box-girder, it will be subjected to compressive membrane stresses. This makes the topic of this section of relevance.

Two types of buckling is of interest when considering SSE's in compression; local buckling of a plate segment (e.g. deck plate between two folds of a corrugated core) and global buckling of the entire sandwich plate. Also a combination of both buckling modes can be relevant.

Buklum et al. [48] and Buklum and Amdahl [49] derived a simplified method for determining buckling strength of stiffened plates. Local buckling is considered separately in a local model and then implemented in a global model. Together, these two models provide an ultimate limit state estimate for design with regards to global buckling.

An analytical expression for the elastic critical global buckling load was presented e.g. by Zenkert, considering an orthotropic sandwich plate including the effect of shear deformations [50].

Nordstrand derived an equation for buckling load of simply supported orthotropic linear elastic plates including first order shear deformation theory. When this theory assessed a shear stiffness that approaches infinity, the result converges towards the buckling load of an orthotropic plate without regards to shear deformation. This implies model accuracy [51].

Local buckling of a plate segment can occur by either compressive membrane stresses perpendicular or parallel to the core or shear stress. Interaction between the stress components is also possible. These critical buckling stresses was presented e.g. by Romanoff and Kujala [52].

#### 3.4.1 Web-core sandwich plate

Figure 32 displays the cross section of a web-core SSE.

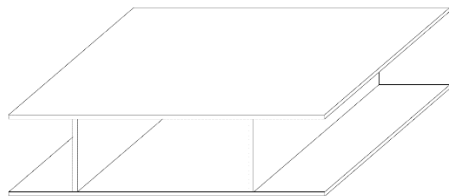


Figure 32. Web-core steel sandwich element [15].

Jelovica and Romanoff present a geometrically non-linear numerical analysis including initial imperfections to display the impact of local buckling on the post-buckling stiffness. The study compares buckling analysis of a full 3-dimensional shell model to an ESL-model. The main difference between the models was that the full 3D analysis captures local deformations. This yields that comparing results from the two models displays the impact of local buckling, and it is shown in Figure 33. This work was performed for a four-edge supported plate either pinned or clamped. Two cross sections were considered: the first with face and web thickness of 2.5mm and 4mm respectively. The second plate had a face and web thickness of 1.5mm and 4mm respectively. The

core height was 40mm and the web spacing 120mm. This puts the cross-section into class 4 of EN 1993-1-1. It was also stated that the most influencing factor on the buckling strength is the transverse shear stiffness in the direction perpendicular to the web longitudinal direction [53].

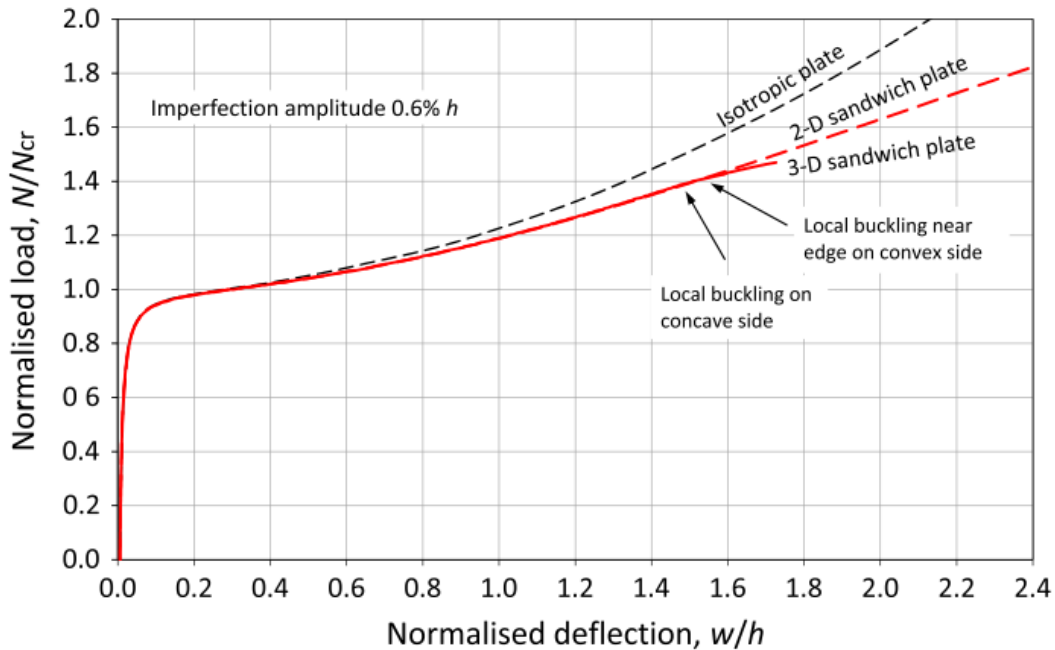


Figure 33. Impact of local buckling on post-buckling stiffness [53].

Figure 33 also shows good agreement between the theory presented by Romanoff et al. [35], used for the case of a single 2D shell, and the 3D numerical model up to the point of local buckling.

The influence of weld rotational stiffness on the buckling strength of a web-core sandwich panel was studied by Jelovica et al. It was shown that the buckling strength was reduced by up to 24% when including the weld rotational stiffness. It was shown to be depending on geometrical aspects and boundary conditions. The strength reduces due to the fact that the rotational stiffness in the connection detail affects the transverse shear stiffness in the direction orthogonal to the web longitudinal direction and further the level of orthotropy [54].

Local buckling was investigated by Kolerts and Zenkert in three companion papers [55], [56], and [57] for web-core steel sandwich elements filled with an adhesively bonded elastomer core. An elastomer-filled web-core sandwich element is shown in Figure 34.

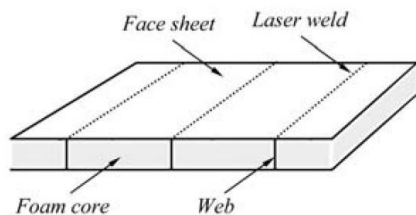


Figure 34. Elastomer-filled sandwich element [55].

The first paper regarded compressive axial force in the direction of the webs. It was concluded that for the elastomer-filled web-core sandwich panel of normal used proportions in ship industry (~40mm web height, 2mm face plates and 4mm web plates spaced 140mm), yielding stress levels were reached before local buckling. An approach for regarding an elastomer core for local buckling phenomenon was introduced too [55].

Kolerts and Zenkert also investigated the elastomer-filled web-core sandwich elements with respect to compressive axial force normal to the web. It was again shown that yielding appears before the system loses stability for cases considered normal in practical use [56].

The third of the three coupled papers of Kolerts and Zenkert regarded ultimate strength and experimental validation. It was shown that the predicted critical load agrees well with non-linear finite element analysis and experimental results [57].

### 3.4.2 Truss-core sandwich beam

Biagi and Bart-Smith investigated the in-plane compressive response of a truss-core sandwich column of stainless steel analytically, numerically and experimentally. The sandwich column was joined by an adhesive brazing process. Analytical formulations were derived including macro buckling, shear buckling and face wrinkling to predict failure mode and create failure mode maps. The considered failure modes and two failure mode maps are shown in Figure 35 and Figure 36 respectively [19].

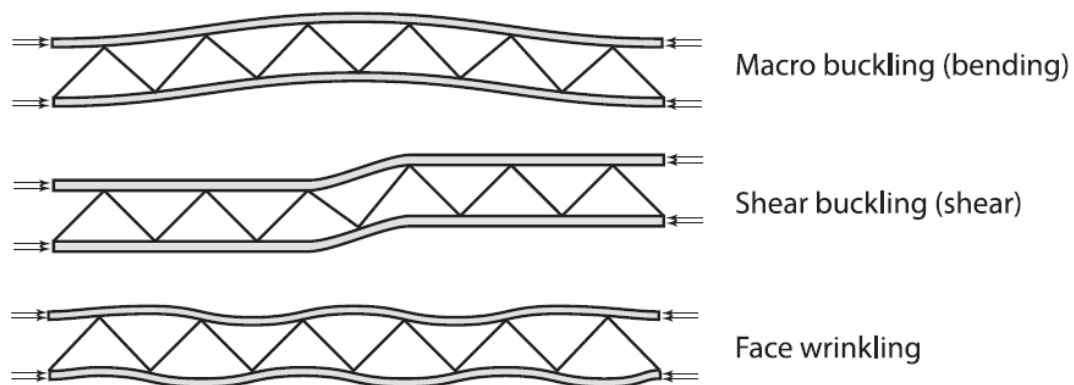


Figure 35. Identified buckling-modes of [19].

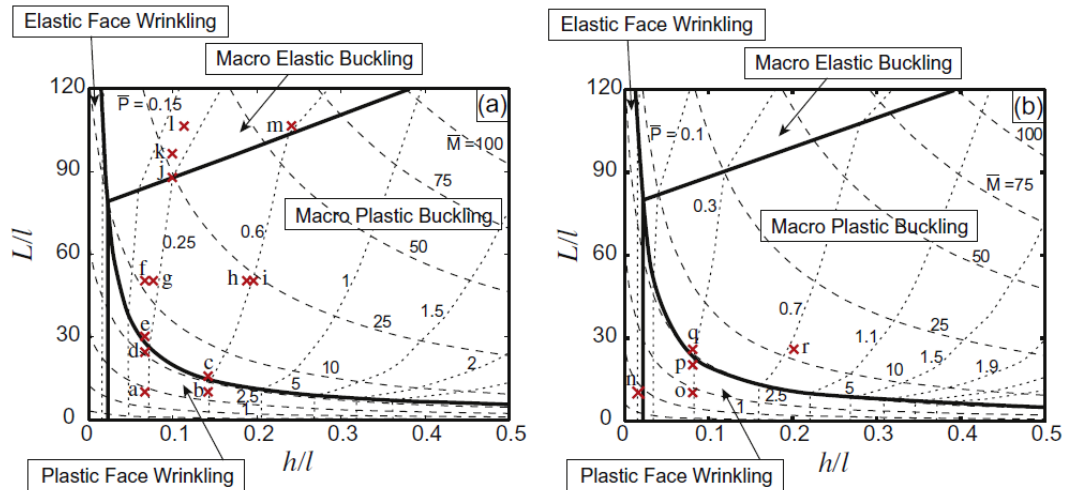


Figure 36. Failure mode maps for a column made of a sandwich element; to the left a more slender column than to the right. [19].

### 3.5 Strength

Romanoff and Kujala summarized strength criteria's for SSE's in a report covering a wide range of perspectives [52]. The following core types was considered: I-core, O-core and V-core, shown in Figure 37.

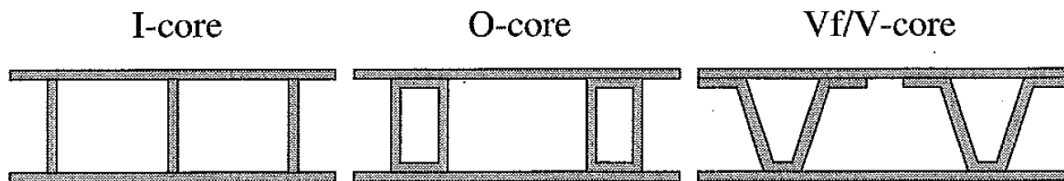


Figure 37. I-core (or web-core), O-core and V-core steel sandwich elements [52].

Loads and load-effects were separated to global and local effects. Where, as an example, a vehicle is regarded globally as a larger surface load and local stresses of the wheel pressure are calculated separately and locally. The work presented Romanoff and Kujala was mainly the result of research at Helsinki ship laboratory and design codes stated by *Det Norske Veritas*. The following design criterias were considered by Romanoff and Kujala [52]:

- Buckling of four edge simply supported orthotropic sandwich plate
- Face plates:
  - o Buckling due to:
    - Membrane stress parallel to the webs
    - Membrane stress orthogonal to the weds
    - In-plane shear stress
    - Interaction between biaxial membrane stress and shear
  - o Patch loads forming dents
  - o Yielding
- Web plate:

- Buckling due to:
  - Pure membrane stress
  - Bending stress
  - Shear stress
  - Interaction between pure membrane – bending – shear
- Yielding
- Plastic collapse due to patch loading

Romanoff and Klanac also presented a summary of strength analysis criteria for filled SSE's [58].

### **3.6 Dynamic response**

Research regarding dynamics of SSE's found in the permits of this work strictly regards impact loading. The dynamic response to intense impulse loads has been studied for sandwich elements by Xue and Hutchinson [59] and Fleck [60]. The studied elements were shown to have high blast resistance.

### **3.7 Patch loading**

Naar presented a model to approximate plastic collapse in the web of a corrugated core SSE due to patch loading [61]. The expressions for plastic collapse are shown by Romanoff and Kujala, but assumptions for the theory is not presented [52].

### **3.8 Optimization**

Optimization can be used for several purposes. For a specific case, it leads to the solution which best fits the optimization target under given constraints. Optimization routines can also be used to display how different parameters in a geometric configuration affects the searched result.

An optimization methodology was introduced by Jefferey et al. using multi-objective genetic optimization. This was done for two cases of through-thickness stake welded V-core sandwich elements under uniformly distributed surface loading in the vertical direction. In their study a geometrically non-linear FEA approach was used. The FEA was verified by existing experimental data. It was shown that this approach is executable for finding the optimum geometric proportions [24].

Frank et al. presented a genetic algorithm based optimization routine that includes integration of different software. This was done for homogenized shell elements to reduce computational time. The considered element was a corrugated core laser stake-welded sandwich element. In a case study presented, a large structural system was optimized with respect to weight, satisfying 297 constraints. It had to run 150 generations of simulations, which took 30 hours of computing time. In the first generation the weight of the structure ranged from 10880 to 11426 kg. The weight of the final structure was 10016 kg. The routine was run under yield and buckling criteria for four different loading conditions [62].

The weight-based optimization performed by Kusters and Wennhage implements the method of moving asymptotes. This was done for the case of laser-welded web-core sandwich elements with an adhesively bonded core. The optimization was shown to

successfully execute its aim. A case study was performed regarding an accommodation deck and girder system. The sandwich deck was simply supported on a girder system and subjected to a design load of  $5 \text{ kN/m}^2$ . Design restrictions regarded: deflection, yielding, core shear, local buckling, local indentation and resonance. This optimization showed that the structural weight of the deck could be reduced by 20%, without utilizing an adhesively bonded core. Furthermore it was shown that another 5% could be saved by injecting a low-cost polyurethane foam and reduce the number of webs. The comparison was made with respect to elements with standard configurations [63].

Optimization of a SSE utilized in a bridge structure would yield understanding of overall impact of geometric configuration on the structural performance.

### **3.9 Design**

It is stated by many authors, for example in SANDCORE, that the most common practice regarding design is to first adopt an analytical model and ESL-approach in an early design stage. This is to evaluate a wide range of geometric possibilities in a direct manner. More detailed numerical analysis can be regarded in a final design stage [8].

## 4 Fatigue performance

Fatigue is often the governing design aspect for steel bridges. If a detail is governed by fatigue, the structure gains nothing from increasing capacity in other limit states. Furthermore, when fatigue is dominant design parameter, high-strength steels are not increasing the load capacity.

### 4.1 Laser-welded joints

Kozak performed strength tests of laser-welded web-core aSSE's and proposed S-N-curves based on fatigue tests. Tests were carried out on different geometries and boundary conditions. For the case of a 3000x1500mm sandwich plate subjected to a centric patch load, fatigue cracks were observed in the weld-toe zone. The cracks propagated from the initiation point in the center of the plate and propagated in the direction of the web-plate. These tests yielded a S-N-curve displayed in Figure 38 [64].

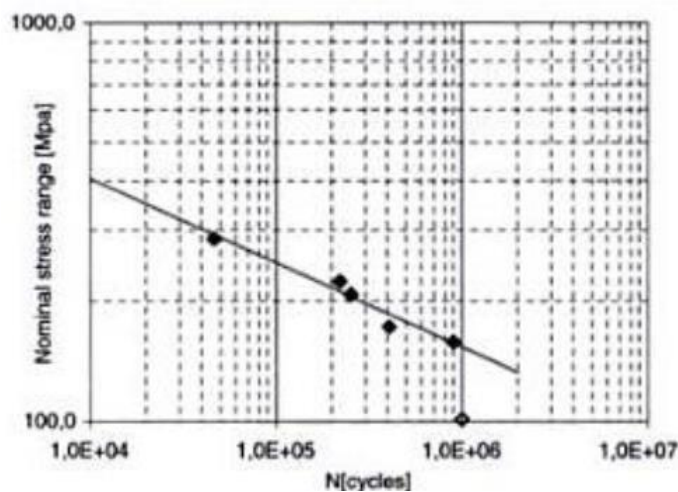


Figure 38. S-N-curve from 3000x1500mm patch-loaded web-core sandwich element [64].

Kozak also tested smaller specimens of 1000x500mm with regards to fatigue and states that they failed in the laser weld due to a moment and shear combined mechanism. Taking into account all tests performed, Kozak states that fatigue cracks for web-stiffened sandwich elements can occur in the following cases [64]:

- case 1: Crack in the laser welded toe in the top plate, in the direction parallel to the web, as a result of the tensile stresses caused by global bending.
- case 2: Crack in the laser welded toe in the top plate, in the direction transverse to the web, as a result of the tensile stresses caused by global bending.
- case 3: Crack in top plate caused by local bending or buckling.
- case 4: Crack in the laser welded contact area of the web and the plates due to transverse bending.
- case 5: Crack in the laser welded contact area of the web and the plates due to longitudinal shear.

Dattoma carried out fatigue tests on over 80 laser-welded austenitic stainless steel specimens in pure tension or shear and reported a smaller HAZ and higher fatigue strength compared to conventional welding [65].

The fatigue strength of laser stake-welded T-joints was investigated by Frank et al. [66]. Geometrical variations, in terms of weld thickness and weld position, was investigated and accounted for in the assessment. These geometrical variations were shown to be normally distributed. Fatigue tests evaluated by Frank et. al. [66] were performed and presented by Socha et al. [67]. Test setup, loading and geometries are shown in Figure 39. Four different test specimens were considered in the tests by Socha et al., shown in Table 2 [67].

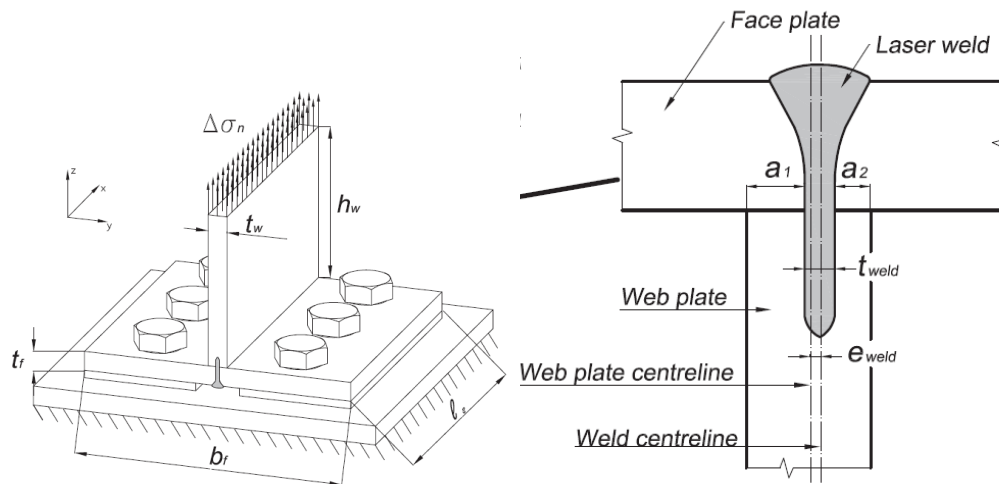


Figure 39. Test setup (left) and specimen geometry (right) [67].

Table 2. Test specimens of [67].

Series	T8x8x24A (FWA)	T8x8x50A (FWB)	T8x8x50L (FWC)	T12x16x24A (FWE)
Thickness of web $t_w$ (mm)	8	8	8	12
Thickness of face plate $t_f$ (mm)	8	8	8	16
Specimen length $l_s$ (mm)	24	50	50	24
Material	A	A	DH36	A
Material yield strength (N/mm <sup>2</sup> )	235	235	355	235
Material ultimate strength (N/mm <sup>2</sup> )	400	400	490	400
No. of specimens	6	6	8	8

Result from the fatigue assessment showed validity in terms of a small scatter band [67]. Three different methods of fatigue assessment were conducted by Frank et. al. J-integral approach,  $r_{ref} = 1$  mm and  $r_{ref} = 0.05$  mm [66]. All the approaches showed alignment with other welded T-joints in terms of fatigue strength for 2 million cycles. However, the  $r_{ref} = 0.05$  mm approach, which was used as a substitute reference radius for thin plates, showed slightly conservative values in comparison to with result from the study.

Bright and Bart-Smith evaluated the fatigue performance for laser stake-welds of a SSE consisting of rolled I-sections as the core. Three weld types were tested; two welds per flange, four welds per flange and two sinusoidal-shaped welds, see Figure 40 to Figure 42, respectively [68].

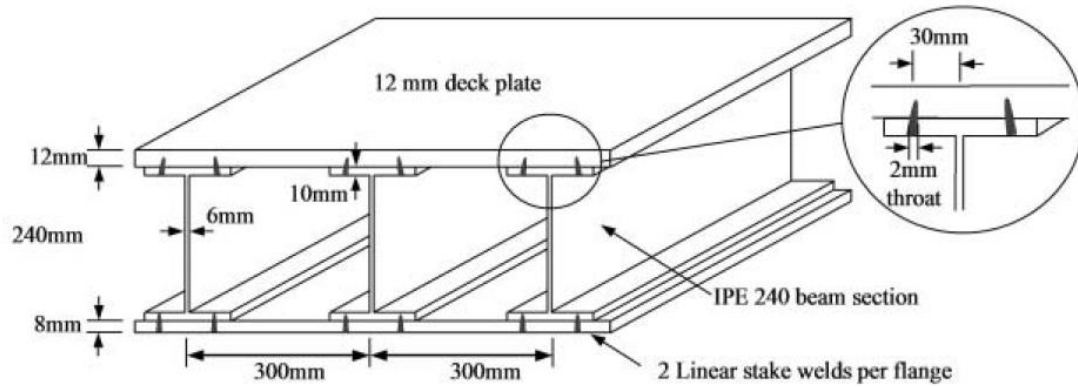


Figure 40. Two welds per flange [68].

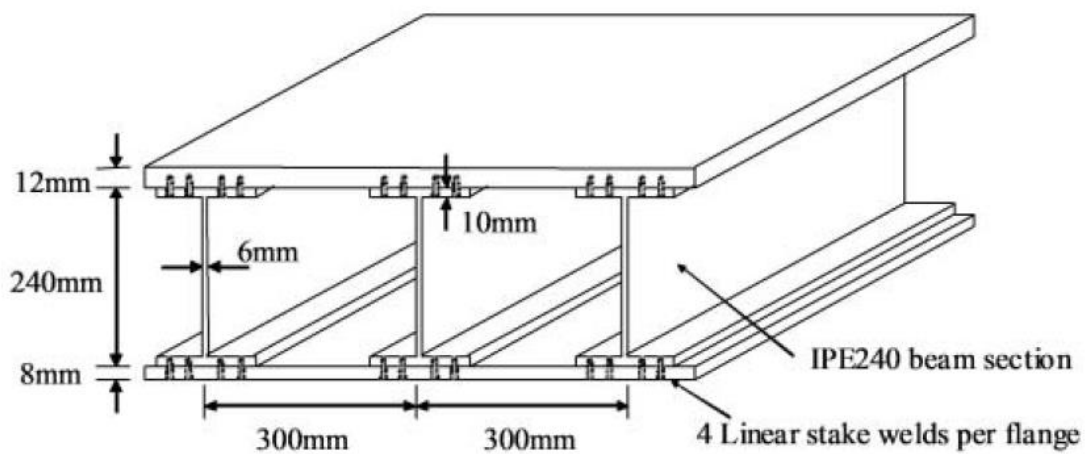


Figure 41. Four welds per flange [68].

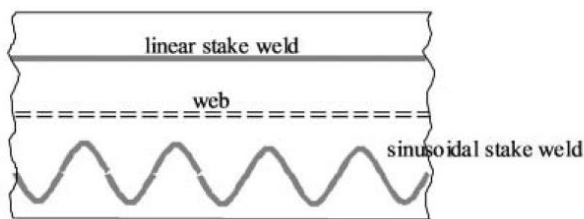


Figure 42. Sinusoidal weld (two welds per flange) [68].

The laser stake-welded sandwich structure was fabricated using a 25kW CO<sub>2</sub> laser source, utilizing 20 kW in this specific production. Two fatigue tests were performed, one regarding uniform deck bending over the center-line of the web and one where lateral deformations were applied to the web of the I-section to resemble offset patch loading, named case 1 and case 2, respectively. The two test loading cases can be seen in Figure 43. Results from the fatigue tests of case 1 (uniform deck bending), which induces shear cracks in the welds, are shown in Figure 44. The test regarding offset patch-load (web bending) did not fail in the weld for any tested specimen. The failure occurred in the root of the web of the rolled I-beam core, see Figure 45 [68].

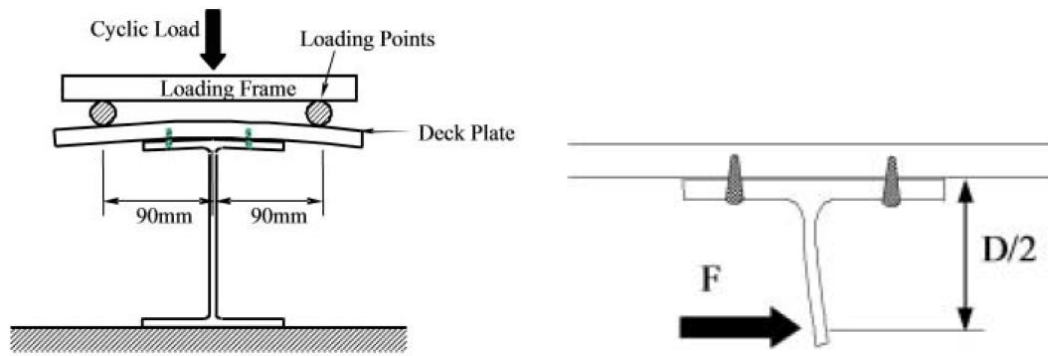


Figure 43. Test setup in the two considered cases of [68].

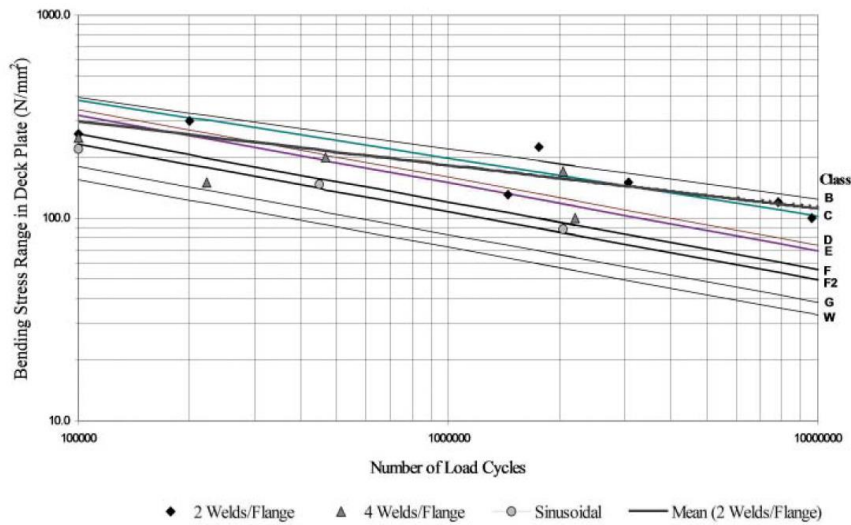


Figure 44. Comparison of fatigue tests to S-N curves of BS 5400. Stress range is regarding bending stresses in the upper face sheet at the position of the welds [68].



Figure 45. Fatigue failure of tests in [68] shown in [2].

Ehlers investigated design of element to element joints with respect to fatigue [69]. To investigate the fatigue behavior, 2D FEA was performed. Five types of joint geometrics were considered and their fatigue notch factor was calculated. Two loading cases were considered: displacement at the edge of the panel (as in Figure 46) and a displacement at the bottom plate. K-factors presented are shown in Figure 47 to Figure 50 in black and grey for the two loading conditions respectively.

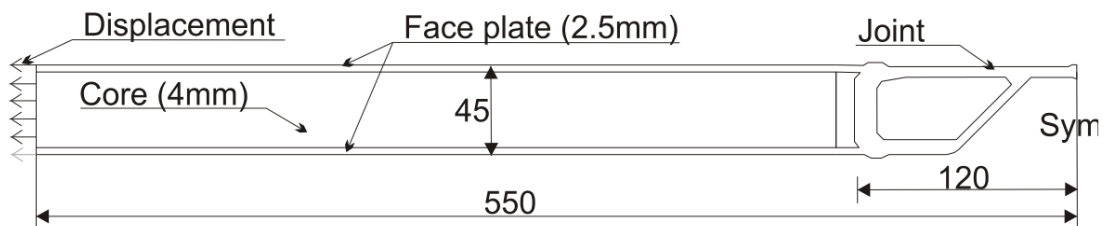
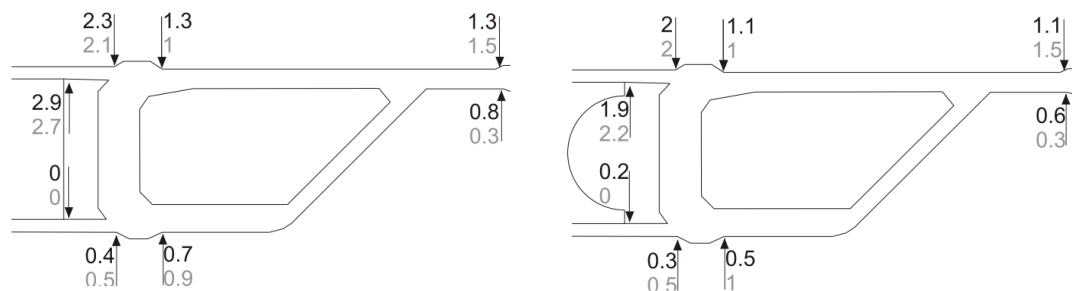


Figure 46. Overview of considered structure [69].



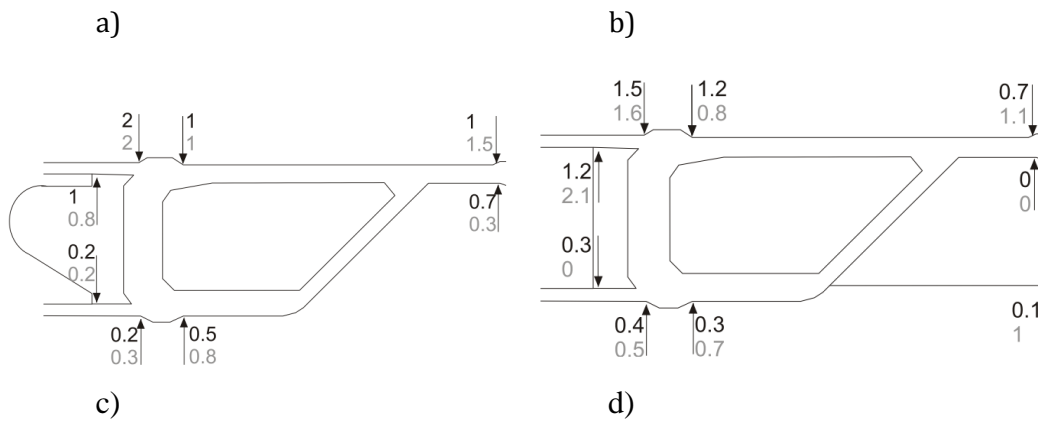


Figure 47. Joint type A, in four different versions [69].

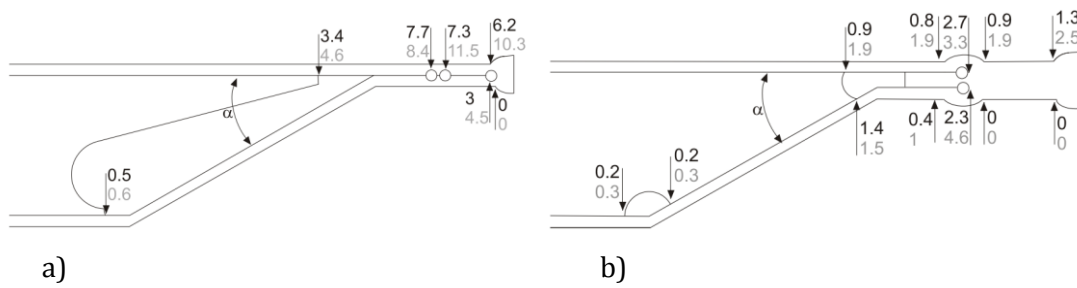


Figure 48. Joint type B, in two different versions [69].

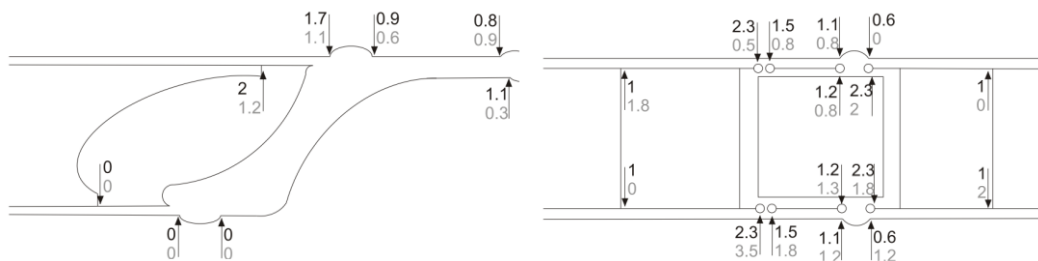


Figure 49. Joint type C (left) and D (right) [69].

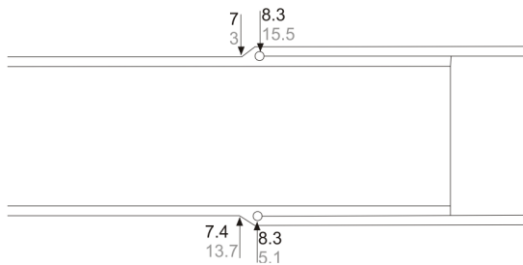


Figure 50. Joint type E [69].

The following was summarized from the investigations:

- Type A with a straight web had a maximum K-factor of 2.9, Figure 47 a)

- Type A with a straight web and a vertical stiffening plate reduced the K-factor to 2.1, but introduced additional welding and production tasks
- Type B induced high overall stresses
- Type C gave good overall results due to optimized shapes
- Type D gave good overall results except from one position
- Type E induced high overall stresses

## 4.2 Hybrid laser-arc welded joints

Caccese et al. performed fatigue testing of HLAW T-joints of various geometrical configurations and stated that the fatigue strength was equal to or greater than conventional welding [70]. Setup for the tests can be seen in Figure 51. The results were compared to conventional welding data of Munse et al. [71] and Kihl [72], see Figure 52.

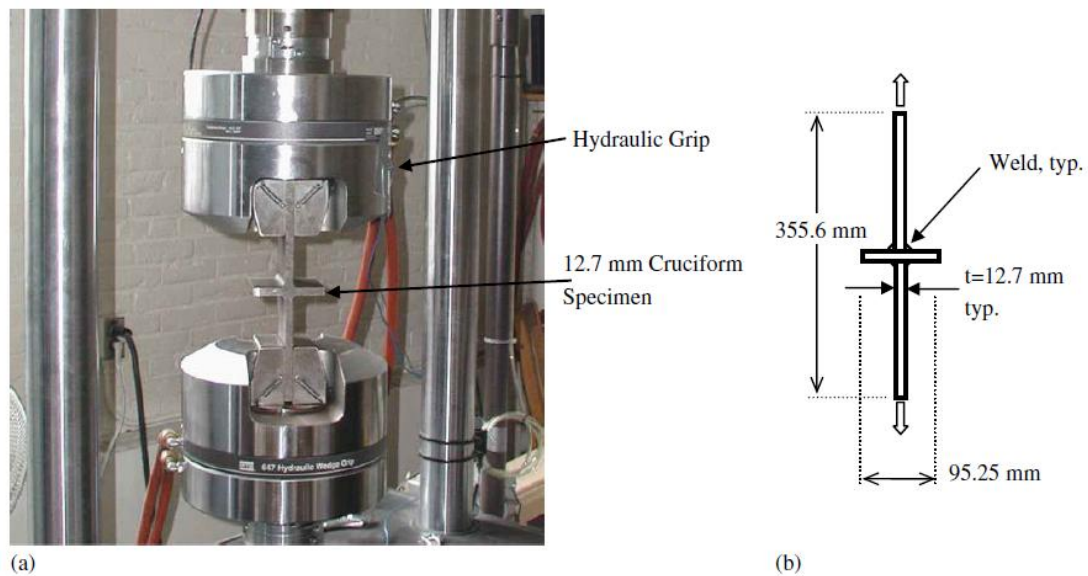


Figure 51. Test setup of studies in [70].

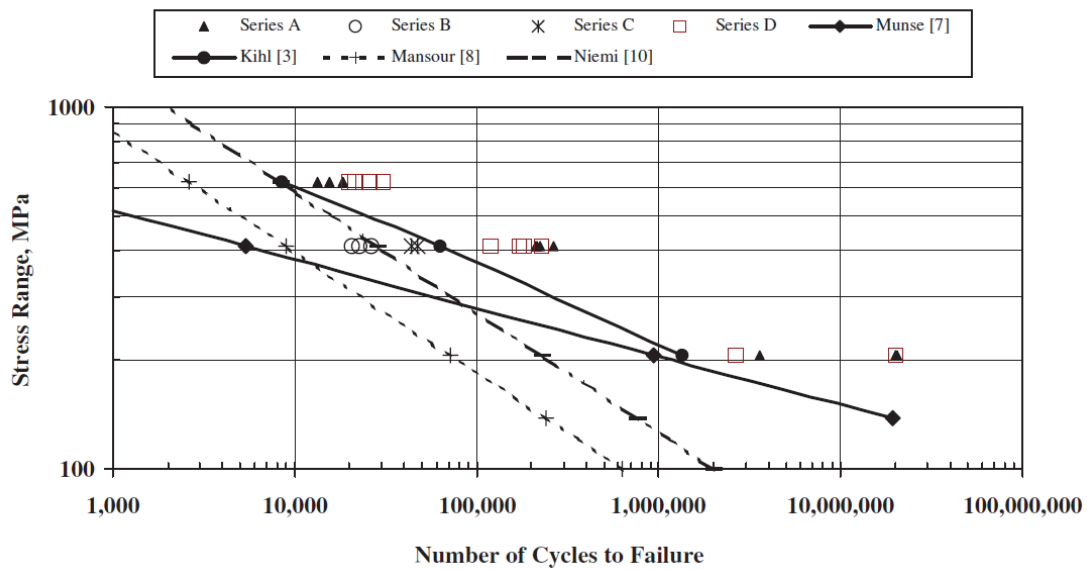


Figure 52. S-N curve of T-joint fatigue tests, series D refer to HLAW and series A to C refer to LW specimens [70].

Remes and Fricke investigated and identified parameters that influence the fatigue strength, based on the structural stress approach [73]. This was done by analyzing the fatigue test data presented Fricke et. al. [74]. The fatigue tests performed by Fricke et. al. are presented in Figure 53 [74].

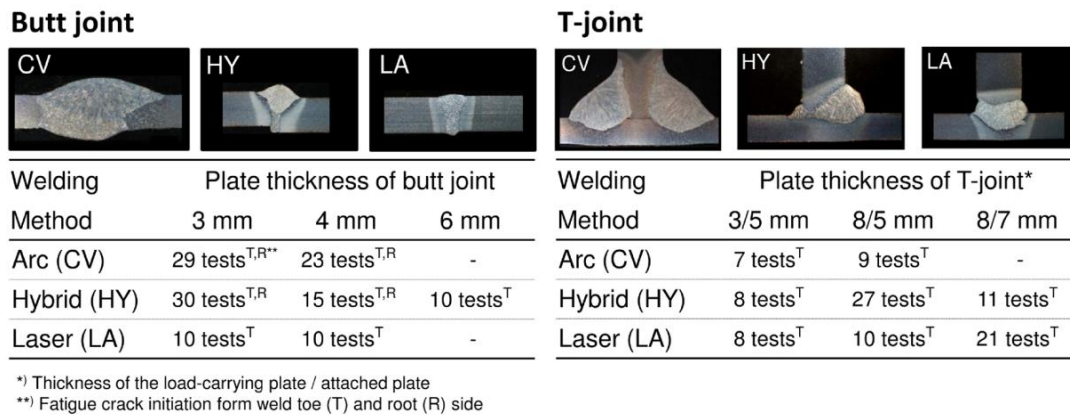


Figure 53. Fatigue test program of [74], presented in [73].

The conclusions drawn by Remes and Fricke are quoted here [73]:

- No beneficial plate thickness effect was observed in butt and T-joints between 3 – 4 and 6 – 8-mm-thick plates.
- Weld quality and particularly undercuts affect thin-plated joints more than thick-plated ones, resulting in larger scatter especially in the high-cycle domain.
- The structural stress approach, in particular the through-thickness linearization, is well-suited for fatigue strength assessment of thin-plated joints.
- The effect of undercuts should be included by determining the structural stress in the net section.

- The 1-mm stress approach by Xiao and Yamada should not be applied to thin-plated joints because the stress location is close to the neutral axis, thus not capturing the secondary bending effect.
- Quality aspects such as misalignments and undercuts play a major part and therefore improved quality may result in higher S-N curves and slope exponents.

Wentzel et al. compared three types of butt-welded connections with respect to, among other things, fatigue. The three weld types can be seen in Figure 54 [30].

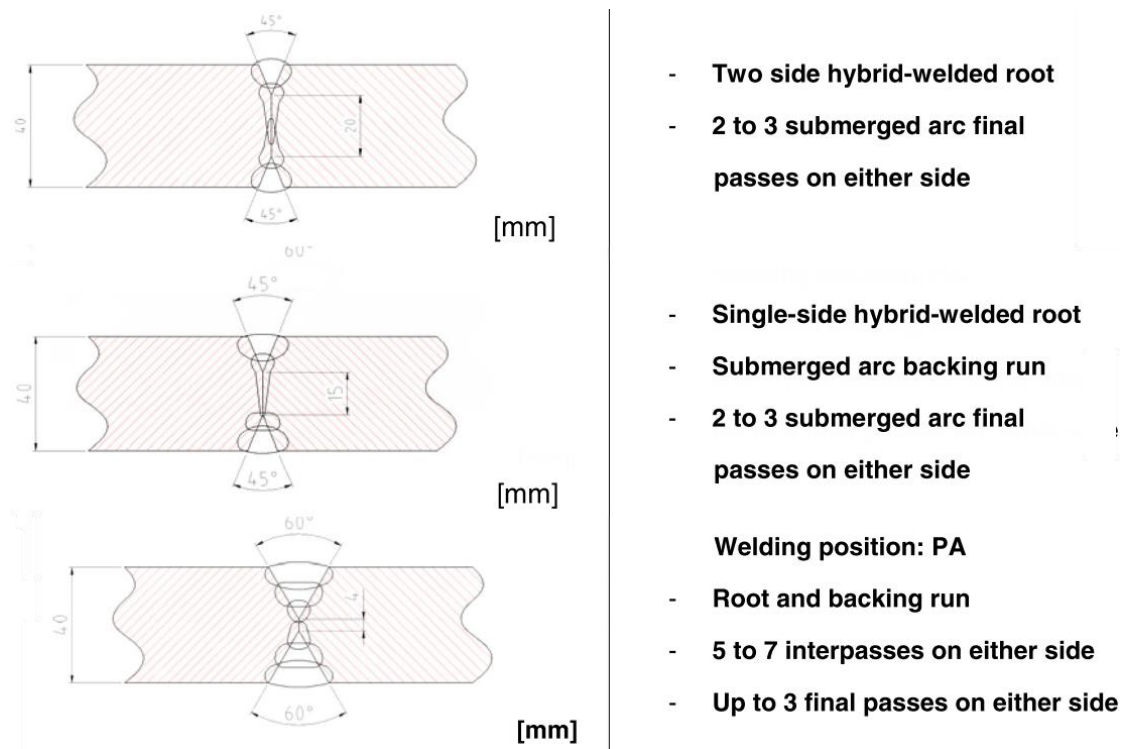


Figure 54. Considered welds of [30]. Double-sided hybrid-weld with submerged arc fill (top), single sided hybrid weld with submerged arc fill (middle) and submerged arc weld solely (bottom) [30].

It was concluded that improvements in fatigue was made in the case of submerged arc-filled laser welds in comparison to the case of submerged arc weld solely. Furthermore, it was shown that this increase was due to geometric properties in the weld rather than the decreased residual stress [30].

## 5 Applications

Application of sandwich elements has been experienced in a range of areas as aviation, aerospace and marine industry.

Abbot et. al. discussed around a research project, called LASCORE that applied a corrugated core SSE in ship building. This was done in the 1980's by the US navy. It yielded a 40% material reduction. However there were no economic gains due to the undeveloped joining techniques [31].

In this section two bridge applications will be considered:

- SSE as a bridge slab in an open cross section and
- Multiple SSEs assembled to a box section.

### 5.1 Bridge slab in open cross section

When the SSE is utilized as a slab for an all-steel bridge it serves locally transferring loads to the supporting structure and as an upper flange in an open cross section carrying the load globally, see Figure 55.

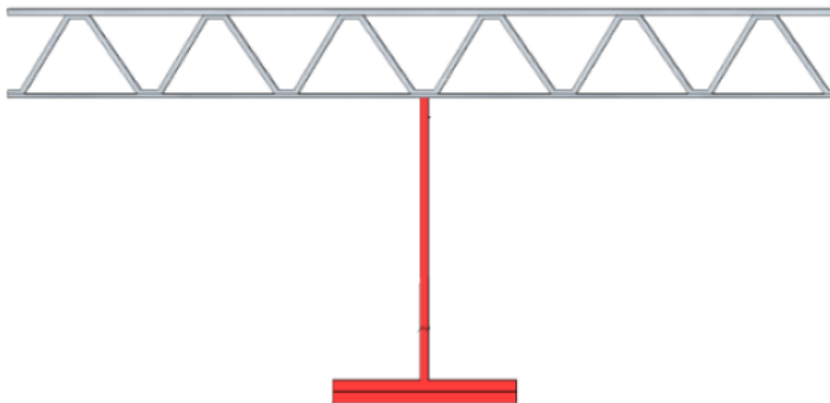


Figure 55. Principle of SSE utilized as bridge slab [5].

#### 5.1.1 General

For this case of application the following gains are achieved in comparison to the conventional orthotropic bridge deck.

- Increased local bending stiffness of the deck in the longitudinal direction of the corrugation or reduced area with equal stiffness i.e. increased local stiffness to weight ratio.
- Increased bending stiffness in the direction transverse to the corrugation.
- Increased global bending stiffness of the girder due to favorable shear lag effects.

#### 5.1.2 Case study

Beneus and Koc [5] performed a case study regarding an open-able all-steel bascule bridge and it will be summarized in this chapter. The regarded bridge was built in 2012 and stretches over Göta canal at Lyrestad, Sweden. It is shown in Figure 56.



Figure 56. Bascule bridge over Göta canal at Lyrestad.

The existing bridge chosen for the case study was conventional for its type and consists of two main girders, 1.8m spaced transverse girders and an orthotropic bridge deck of a steel face plate and longitudinal trapezoidal stiffeners. In the case study the existing bridge was compared to an alternative with steel-sandwich deck. The total cross section height was kept constant. The two compared structures are shown in Figure 57.

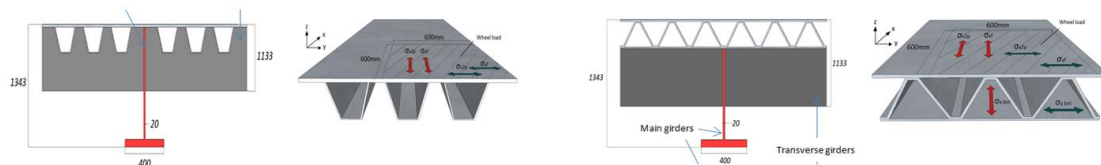


Figure 57. Compared alternatives in [5].

In the initiating stage of the case study an optimization of the bridge deck was performed. Two different optimization aims were introduced. The first regarding minimization of cross sectional area while keeping the bending stiffness constant in the longitudinal direction of the corrugation. The other approach kept the cross sectional area constant with the focus to maximize bending stiffness in the corrugation longitudinal direction. Optimization routines were executed under boundary conditions other than bending stiffness and cross sectional area, regarding fatigue strength, local deformations and local buckling.

The reduction of cross sectional area approach yielded a decrease of material of 23% in the slab element, and was denoted as min A. The increased stiffness approach gave an increase of 82% regarding bending stiffness in the longitudinal direction of the

corrugation. This approach was denoted as max D. The results of this optimization study with yielded material savings and stiffness increase is shown in Table 3. In this case x was the longitudinal direction of the corrugated core and y the direction transversal to the corrugation.

Table 3. *Bending stiffness ( $D_x$  and  $D_y$ ), torsional stiffness( $D_{xy}$ ) and area for the Steel sandwich deck (SSD) and orthotropic deck (Ortho) [5]*

	<b>Max <math>D_x</math></b>				<b>Min A</b>			
	$D_x$ [Nm]	$D_y$ [Nm]	$D_{xy}$ [Nm]	Area [m <sup>2</sup> /m]	$D_x$ [Nm]	$D_y$ [Nm]	$D_{xy}$ [Nm]	Area [m <sup>2</sup> /m]
SSD	6.407e7	4.884e7	3.671e7	0.03	3.531e7	2.664e7	2e7	0.024
Ortho	3.531e7	1.186e7	2.046e7	0.03	3.531e7	1.186e7	2.046e7	0.03
Ratio	82%	312%	79%	0%	0%	125%	0%	-23%

To further investigate the total gains on a full system level the three alternatives were evaluated numerically in a finite element analysis (FEA). From the global FEA the longitudinal bending stresses in the main girders where, for both cases below 50 % of the conventional orthotropic case. This has two reasons earlier mentioned. Load spreading effects due to low level of orthotropy and shear-lag effects. Compared shear-lag effects in terms of effective widths are shown in Table 4.

Table 4 *Effective flange width for the three bridge models, with utilization ratios [5].*

Cross section	$b_{eff}$ [mm]	Utilization ratio $b_{eff}/b$ [%]
Max $D_x$	4027	66
Min A	3405	59
Ortho	2427	37

The FEA showed possibilities to reduce steel amounts further. This was done by removing every other cross beam and reducing the thickness of the bottom flange of the main girder. The total reduced amount of steel was 44% for the minA alternative, still with lower stress levels than for the conventional orthotropic bridge alternative.

The results of the case study performed by Beneus and Koc is aligned with the statements of Chapter 3.3.

## 5.2 Box girder cross section

This section regards the use of SSE's in box-girder sections, utilized in long-span bridges i.e. cable-supported bridges. All-steel cross sections are used in this kind of structures due to its high stiffness to weight ratio.

In the case of application as a slab in an open cross section, the structural performance is enhanced by all the factors of Chapter 3.3. For the case of a box girder in a cable-supported bridge, the shear-lag effects are less significant. A schematic sketch of a box section composed of SSE's is shown in Figure 58.

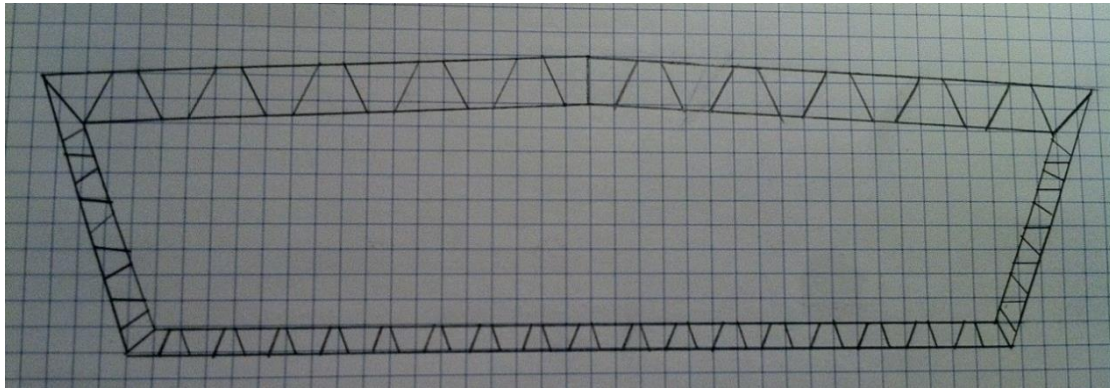


Figure 58. Schematic of box-girder composed of steel-sandwich elements.

Reducing the cross sectional area in the principally same manner as for the slab open cross section application will affect the girders supporting structure and the erection phase.

In long-span cable-stayed bridges the cables suffer from insufficiency due to sagging effects when increasing the cable length. The sag is proportional to the square of the weight of the material used in the cable. It is also independent of the cross sectional area of the main cable. It is also inverted proportional to the stress in the cable. Thus, decreasing the weight of the stiffening girder reduces the needed cable area, but has no impact on the efficiency level for the cable i.e. a reduced load on the cable does not increase the maximum theoretical span length.

In the case of suspension bridges the theoretical maximum static span width was shown for example in [75]. It was shown to have a dependency of the load acting on the main cable, i.e. the weight of the supporting girder affects the maximum theoretical span length.

The deck of a stiffening girder is often far wider than the distance between diaphragms. To utilize the less orthotropic behavior in a steel sandwich deck, the length to distance between diaphragm-ratio shall be closer to 1. Furthermore the geometric configuration normally used induces buckling in a column-like manner. To gain from the post buckling strength of the less orthotropic sandwich deck, the mentioned ratio also needs to be closer to 1.

## 6 Further research

This chapter will in general terms point out some of the topics of this report that needs further research, for the case of SSEs in bridge applications. The corrugated core SSE is the base for these conclusions.

### *Fatigue*

- The fatigue strength of the corrugated core SSE HLAW connection detail is unknown, and needs further research

### *Production*

- The feasibility of joining a steel sandwich element using LW and HLAW is known
- Welding parameters of HLAW and their impact on residual stress and deformation for a corrugated core sandwich element needs further research
- Longitudinal and transversal joints for bridge application steel sandwich elements needs further research

### *Bending behavior*

- Cross sectional parameters of the corrugated core SSE is known
  - o The case of multiple weld beads per horizontal part of the core needs further research. It has an impact on the transversal shear stiffness in the direction perpendicular to the core.
  - o For the case on one single weld, weld rotational stiffness need further research. It has an impact on the transversal shear stiffness in the direction perpendicular to the core.
- Plate theories to estimate averaged plate deflections exist
  - o Theories to predict accurate stress levels due to global and local effects exists for the web-core SSE.
  - o Plate theories to predict accurate stress levels due to global and local effects needs further research.

### *Shear-lag*

- Shear-lag effects for corrugated core SSEs need further research. They need to be quantified and simplified engineering methods are needed.

### *Stability*

- Analytical elastic critical buckling loads can be calculated for the case of a orthotropic plate including the effect of shear deformations
  - o Further research is needed regarding ultimate compressive strength for corrugated core SSE.
    - This topic is especially crucial for cable supported box section stiffening girders.

### *Patch-loading*

- An approximate expression for patch-loading capacity of an inclined core plate exists. This expression need to be validated. If it is not appropriate for use in design, further research is needed.

## References

- [1] World Steel Association. (2014). *World steel in figures 2014*. URL 2014-11-14: <http://www.worldsteel.org/dms/internetDocumentList/bookshop/World-Steel-in-Figures-2014/document/World%20Steel%20in%20Figures%202014%20Final.pdf>
- [2] Bright, S.R and Smith, J.W. (2007). *A new design for steel bridge decks using laser fabrication*. The structural engineer, volume 85, issue 21, ISSN: 1466-5123
- [3] Wolchuck, R. (1963). *Design manual for orthotropic steel plate deck bridges*. New York: American Institute of Steel Construction.
- [4] [http://commons.wikimedia.org/wiki/File:1985\\_redecking\\_work,\\_Steel\\_Bridge,\\_Portland.jpg](http://commons.wikimedia.org/wiki/File:1985_redecking_work,_Steel_Bridge,_Portland.jpg), 2015-05-07
- [5] Beneus, E. & Koc, I. (2014). *Innovative Road Bridges with Steel Sandwich Decks*. Göteborg: Chalmers University of Technology.
- [6] <http://www.mtc.ca.gov/news/photos/paiva.htm>, 2015-05-07
- [7] Kenno Tech. (n.d.). *A lighter future for structures*. Retrieved May 29, 2014, from Kenno Tech Web Site: [www.kennotech.fi](http://www.kennotech.fi)
- [8] SANDCORE. *Best Practice Guide for Sandwich Structures in Marine Applications*. Prepared by the SAND.CORE Co-ordination Action on Advanced Sandwich Structures in the Transport Industries Under European Commission Contract No. FP6-506330.
- [9] Kolstein M, H. (2007). *Fatigue classification of welded joints in orthotropic steel bridge decks*. Doctoral thesis. TU Delft.
- [10] Wolchuk, R. (1990) Lessons from weld cracks in orthotropic decks on three European bridges. ASCE J. Structural engineering 116/1
- [11] Ya, S. et al. (2011). *Fatigue Evaluation of Rib-to-Deck Welded Joints of Orthotropic Steel Bridge Deck*. Journal of bridge engineering 16/4. pp 492-499.
- [12] Säynäjäkangas, J and Taulavuori, T. (2004) *A review in design and manufacturing of stainless steel sandwich panels*. <http://www.stainless-steel-world.net/>, 2004.
- [13] Kujala, P and Klanac, A. *Steel Sandwich Panels in Marine Applications*. Shipbuilding 65/4 2005.
- [14] Hoffart, J and Hansen, E. (2008). *Design implications of sandwich panels*. Pentons welding magazine 81/10. pp 27-30.
- [15] Romanoff, J. (2007). *Bending Response of Laser-Welded Web-Core Sandwich Plates*. Doctoral dissertation. Helsinki University of Technology. ISBN: 978-951-22-8976-9.
- [16] Alwan, U. & Järve, D. (2012). *New Concept for Industrial Bridge Construction*. Göteborg: Chalmers University of Technology.

- [17] Roland, F and Reinert, T. (2000) *Laser welded sandwich panels for the shipbuilding industry*. At: <http://sandwich.balport.com/downloads/Kurz.PDF> 2014-11-13. 2000.
- [18] Kujala et. al. (2004). *All steel sandwich panels – Design challenges for practical applications on ships*. 9<sup>th</sup> symposium on practical design of ships and other floating structures, Luebeck – Travemunde, Germany.
- [19] Biagi, R. & Bart-Smith, H. (2012). *In-plane column response of metallic corrugated core sandwich panels*. International Journal of Solids and Structures 49 p. 3901-3914.
- [20] Caccese, V and Yorulmaz, S (2009). *Laser Welded Steel Sandwich Panel Bridge Deck Development: Finite Element Analysis and Stake Weld Strength Tests*.
- [21] Baker, M, A. (2011). *Gas Metal Arc Welding*. Hobart Institute of Welding Technology. ISBN 978-1-936058-17-4.
- [22] [http://www.substech.com/dokuwiki/doku.php?id=metal\\_inert\\_gas\\_welding\\_mig\\_gmaw&s=gas%20metal%20arc%20welding](http://www.substech.com/dokuwiki/doku.php?id=metal_inert_gas_welding_mig_gmaw&s=gas%20metal%20arc%20welding), 20150223, 12:50.
- [23] Denney, P. (2011) *Hybrid laser arc welding: Has its time arrived?* URL: <http://www.industrial-lasers.com/articles/print/volume-26/issue-1/features/hybrid-laser-arc-welding-has-its-time-arrived.html>. 2014-11-14.
- [24] Jefferey et. al. (2013). *Multi-objective optimization of laser-welded steel sandwich panels for static loads using a genetic algorithm*. Eng. Str. 49. p. 508-524.
- [25] SANDWICH (2000) *Advanced composite sandwich steel structures*. URL: [http://sandwich.balport.com/public\\_downloads/public-project-summary.pdf](http://sandwich.balport.com/public_downloads/public-project-summary.pdf). Captured 2012.
- [26] Lankalaoalli, K N. Tu, J F. Gartner, M. (1996). *A model for estimating penetration depth of laser welding processes*. Journal of Physics D: Applied Physics 29. pp 1831-1841.
- [27] Miller, C.B. (nd) *Laser welding article* URL: <http://www.uslasercorp.com/envoy/welding.html>. 2014-11-14.
- [28] Defalco, J. (2007), *Practical Applications for Hybrid Laser Welding*, WELDING JOURNAL October 2007.
- [29] ESAB. (2010). *Joint Specifications for Hybrid Laser Arc Welding Applications*. Presentation 2010-03-29.
- [30] Wetzel, G. et al. (2014). *Investigation of properties in hybrid welds at 40mm sheet thickness*. Welding in the World 58. pp 883-891.
- [31] Abbott, S.P., et al. (2007). *Automated Laser Welded High Performance Steel Sandwich Bridge Deck Development*. TRB 2008 Annual Meeting.
- [32] Jelovica, J. (2014). *Global buckling response of web-core steel sandwich plates influenced by general corrosion*. Aalto University. Doctoral dissertation. ISBN: 978-952-60-5860-3
- [33] Karol, N. (2008). *Search for optimum geometry of selected steel sandwich panel joints*. Polish maritime research 15. pp 26-31.

- [34] Kozak, J. (2009). *Selected problems on application of steel sandwich panels to marine structures*. Polish maritime research 16. pp 9-15.
- [35] Romanoff, J., and Varsta, P. (2006). *Bending response of web-core sandwich beams*. Composite Structures 73.
- [36] Libove, C. and Batdorf, S.B. (1948). *A General Small-Deflection Theory for Flat Sandwich Plates*. NACA TN 1526, Langley Memorial Aeronautical Laboratory, Langley Field, Va
- [37] Romanoff J, Varsta P. (2007). *Bending response of web-core sandwich plates*. Composite Structures, 81/2, pp. 292-302.
- [38] Nordstrand, T. (2004). *Analysis and testing of corrugated board panels into the post-buckling regime*. Composite structures 63. p. 189-199.
- [39] Romanoff, J. Remes, H. Socha, G. Jutila, M. and Varsta, P., (2007). *The Stiffness of Laser Stake Welded T-joints in Web-core Sandwich Structures*. Thin-Walled Structures. Vol. 45. pp. 453–462.
- [40] Libove, C & Hubka, R E. (1951). *Elastic constants for corrugated-core sandwich plates*. 1951. NACA Tech. note 2289.
- [41] Chang et al. (2004). *Bending behavior of corrugated-core sandwich plates*. Composite Structures 70. p. 81–89
- [42] Lok, T., & Cheng, Q. (1999). *Elastic Deflection of Thin-Walled Sandwich Panel*. Journal of Sandwich Structures and Materials, 1-279.
- [43] Tan et. al. (1989). *Steel sandwich panels: finite element, closed solutions and experimental analysis on a 6x2m panel*. The structural engineer 67/9. p. 159-166.
- [44] Lok, T-S. Cheng, Q-H. (2000). *Elastic stiffness properties and behavior of truss-core sandwich panel*. J. Struct. Eng 126. p 552-559.
- [45] Cheng et al. (2005). *A numerical analysis approach for evaluating elastic constants of sandwich structures with various cores*. Composite Structures 74. p. 226–236.
- [46] Pantsar, H. et al. (2004). *Quality and costs analysis of laser welded all steel sandwich panels*. Journal of Laser Applications 16. pp. 66-72.
- [47] Romanoff J., (2011). *Interaction between laser-welded web-core sandwich deck plate and girder under bending loads*. Thin-walled structures, 49, pp 772-781.
- [48] Byklum, E. et al. (2004). *A semi-analytical model for global buckling and postbuckling analysis of stiffened panels*. Thin-walled structures 42. p 701-717.
- [49] Byklum, E and Amdahl, J (2002). *A simplified method for large deflection analysis of plates and stiffened panels due to local buckling*. Thin-walled structures 40. p 925-953.
- [50] Zenkert, D. (1995). *An Introduction to Sandwich Construction*. Engineering materials advisory services.
- [51] Nordstrand, T. (2004). *On buckling loads for edge-loaded orthotropic plates including transverse shear*. Composite structures 64. p. 1-6.

- [52] Romanoff, J. and Kujala, P. (2002). *Formulations for the strength analysis of all steel sandwich panels*. Report Helsinki ship laboratory. M-266.
- [53] Jelovica, J. & Romanoff, J. (2013). *Load-carrying behaviour of web-core sandwich plates in compression*. Thin-walled structures 73. p 264-277.
- [54] Jelovica, J. Romanoff, J. Ehlers, S. Varsta, P. (2012). *Influence of weld stiffness on buckling strength of laser-welded web-core sandwich plates*. Journal of constructional steel research 77. p 12-18.
- [55] Kolsters, H and Zenkert, D. (2006). *Buckling of laser-welded sandwich panels. Part 1: elastic buckling parallel to the webs*. Journal of mechanical engineering for the maritime environment 220/67. p 67-79.
- [56] Kolsters, H and Zenkert, D. (2006). *Buckling of laser-welded sandwich panels. Part 2: elastic buckling normal to the webs*. Journal of mechanical engineering for the maritime environment 220/81. p 81-94.
- [57] Kolsters, H and Zenkert, D. (2009). *Buckling of laser-welded sandwich panels: ultimate strength and experiments*. Journal of Engineering for the Maritime Environment. Vol. 224. pp 29-45.
- [58] Romanoff, J. and Klanac, A. (2004). *Design formulations for filled structural sandwich panels*. Report Helsinki ship laboratory. M-288.
- [59] Xue, Z & Hutchinson, J W. (2004). *A comparative study of impulse-resistant metal sandwich plates*. International Journal of Impact Engineering 30. p 1283–1305
- [60] Fleck, N A. (2004). *The Resistance of Clamped sandwich beams to shock loading*. Journal of Applied Mechanics 71. P. 386-401.
- [61] Naar. H. (1997). *All Steel Corrugated Core Sandwich Panels under Patch Loading*. Diploma thesis. Helsinki University of Technology, Ship Laboratory.
- [62] Frank, D. et Al. (2010). *Optimization system for design of laser-welded steel-sandwich structures*. 11th Symposium on Practical Design of Ships and Other Floating Structures - PRADS 2010, At Rio de Janeiro, Brasil.
- [63] Kolsters, H. and Wennhage, P. (2009). *Optimisation of laser-welded sandwich panels with multiple design constraints*. Marine structures 22. pp 154-171.
- [64] Kozak, J. (2005). Strength tests of steel sandwich panel. Maritime transportation and exploitation of ocean an costal resources – Guedes Soares, Garbatov and Fonseca.
- [65] Dattoma, V. (1994). *Prediction of laser welded stainless steel joints*. Fatigue Fract. Eng Mater. Struct. 17/11. pp. 1335-1342
- [66] Frank, D. et al. (2011). *Fatigue assessment of laser stake-welded T-joints*. International Journal of Fatigue 33. pp 102-114.
- [67] Socha, G. et al. (1998). *Mechanical tests and metallurgical investigation on weld samples*. Report AWCS – Project No. BE 96-3932 – Task A4.
- [68] Bright, S.R and Smith, J.W. (2009). Fatigue performance of laser-welded steel bridge decks. The structural engineer 82/21. pp 31-39.
- [69] Ehlers, S. (2006). *Design of Steel Sandwich Panel Joints with Respect to Fatigue Life*, STG Band 98, ISBN 3-540-27423-5.

- [70] Caccese et al. (2006) *Effect of weld geometric profile on fatigue life of cruciform welds made by laser/GMAW processes*. Mar Struct J 19. p. 1–22.
- [71] Munse WH, W. T. (1983). *Fatigue characterization of fabricated ship details for design*. Springfield: Ship Structure Committee.
- [72] Kihl, D.P. (2002). *Fatigue Strength of HSLA-65 Weldments*. Naval Surface Warfare Center – Carderock Division; Survivability, Structures, and Materials Directorate Technical Report.
- [73] Remes, H. and Fricke, W. (2014). *Influencing factors of fatigue strength of welded thin plates based on structural stress assessment*. Weld World 58. pp 915-923.
- [74] Fricke W, Remes H, Feltz O, Lillemäe I, Tchuindjang D, Reinert T, Nevierov A, Sichermann W, Brinkmann M, Kontkanen T, Bohlmann B, Molter L (2013) *Fatigue strength of laser-welded thin plate ship structures based on nominal and structural hot-spot stress approach*. Proc. of 4th Int. Conf. on Marine Structures (MARSTRUCT ' 2013). Guedes Soares C, Romanoff J (Eds). Taylor & Francis, London. pp 249 – 254
- [75] Banck, F. & Rosén, O. (2014). *Application of CFRP Cables in Super Long Span Cable Supported Bridges*. Göteborg: Chalmers University of Technology.

## Appendix A

Figure A1 is shown to give the geometry and coordinate system for equations 1 – 11.

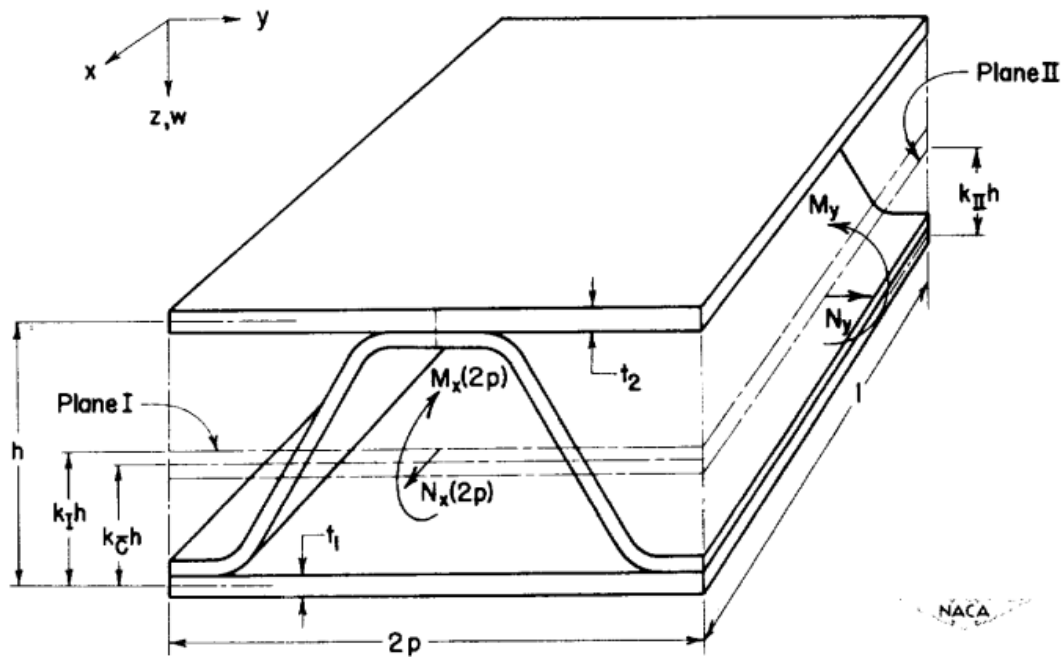


Figure A1. Coordinate system coupled to equation 1 – 11 [22].

$$I_f = \frac{1}{2} t_f h^2 \quad (1)$$

$$D_x = E_c I_c + E_f I_f \quad (2)$$

$$D_y = \frac{E_f I_f}{1 - \nu_f^2 \left(1 - \frac{E_f I_f}{D_x}\right)} \quad (3)$$

$$D_{xy} = 2G_f I_f \quad (4)$$

$$A_f = 2t_f \quad (5)$$

$$E_x = E_c A_c + E_f A_f \quad (6)$$

$$E_y = \frac{E_f A_f}{1 - \nu^2 \left(1 - \frac{E_f A_f}{E_x}\right)} \quad (7)$$

$$G_{xy} = \frac{G_c t_c^2}{A_c} + 2G_c t_f \quad (8)$$

$$D_{Qy} = Sh \left( \frac{E_c}{1 - \nu_c^2} \right) \left( \frac{t_c}{h_c} \right)^3 \quad (9)$$

$$A_c = \frac{l_c t_c}{p} \quad (10)$$

$$D_{Qx} = \frac{G_c t_c^2}{A_c} \left(\frac{h}{p}\right)^2 \quad (11)$$

Where:

$I_f$	Moment of inertia of face sheets	[m <sup>4</sup> /m]
$I_c$	Moment of inertia of the core	[m <sup>4</sup> /m]
$A_f$	Cross sectional area of face sheets	[m <sup>2</sup> /m]
$A_c$	Cross sectional area of the core	[m <sup>2</sup> /m]
$t_f$	Flange thickness	[m]
$t_c$	Thickness of corrugated-core sheet	[m]
$h$	Distance between centre of gravity of flanges	[m]
$h_c$	Distance between the centre planes of the face sheets	[m]
$D_x$	Bending stiffness in the x-direction	[Nm <sup>2</sup> /m]
$D_y$	Bending stiffness in the y-direction	[Nm <sup>2</sup> /m]
$D_{xy}$	Torsional stiffness of the xy-plane	[Nm/m]
$D_{Qx}$	Transverse shear stiffness parallel to the corrugation axis	[N/m]
$D_{Qy}$	Transverse shear stiffness perpendicular to the corrugation axis	[N/m]
$E_c$	Modulus of elasticity of the core material	[Pa]
$E_f$	Modulus of elasticity of face sheet material	[Pa]
$\nu_f$	Poisson's ratio of face sheet material	[-]
$E_x$	Axial stiffness in the x-direction	[N/m]
$E_y$	Axial stiffness in the y-direction	[N/m]
$G_{xy}$	Shear stiffness in the horizontal direction	[N/m]
$G_c$	Shear modulus of elasticity of core material	[Pa]
$G_f$	Shear modulus of elasticity of face sheet material	[Pa]
$\nu_c$	Poisson's ratio of core material	[-]
$S$	Non-dimensional coefficient	[-]
$l_c$	Length of one corrugation leg measured along the centre line	[m]
$p$	Half of the corrugation pitch	[m]